[49]See Ref. 18, Fig. 2, for an example.

[50]The cross section for $N_2^+ + N_2 \rightarrow N_2 + N_2^+$ is in very good agreement with the same cross section measured by J. J. Leventhal, T. F. Moran, and L. Friedman, J. Chem. Phys. 46, 4666 (1967).

[51]See Ref. 1, p. 662ff; the factor f is not in Eq. (101) on p. 663, but is in Eq. (107) on p. 667. See also Ref. 41. Particular states of A^+ and B may give rise to several electronic states of the AB^+ molecule. f is the probability that the colliding atoms A^+ and B approach each other along an A^+B potential curve (Ref. 36) which crosses an appropriate potential curve for B^+A at a point such that dissociation into B^+ and A is possible.

[52]It is here assumed that $(l+\frac{1}{2})^2/R^2 = 0$ when $l = 0$ and that $x = \infty$ when $l = L$; compare Eqs. (101) and (108) in Chap. XIX of Ref. 1.

PHYSICAL REVIEW A VOLUME 5, NUMBER 3 MARCH 1972

Electronic Transitions in Slow Collisions of Atoms and Molecules. IV. Multistate Eikonal Approximation for Quasiadiabatic Transitions*

Joseph C. Y. Chen
Department of Physics and Institute for Pure and Applied Physical Sciences, University of California, San Diego, La Jolla, California 92037
and
Charles J. Joachain† and Kenneth M. Watson
Department of Physics and Lawrence Radiation Laboratory, University of California, Berkeley, California 94720
(Received 26 July 1971)

The coupled equations of the adiabatic-state expansion method for quasiadiabatic transitions in atomic collisions are reduced in the eikonal approximations to a form that allows straightforward computation. The multistate eikonal approximation is then applied to the $He^+(1s) + H(1s) \rightarrow He^+(1s) + H(2p)$ excitation process. The partial and total $2p$-excitation cross sections as well as the polarization of the light emitted by the excited H atoms are calculated. Our results compare well with recent experimental measurements. The importance of final-state coupling is dramatically illustrated by the above $2p$-excitation process. The qualitative features of the nonadiabatic effects are also investigated in the eikonal Born approximation as functions of the position and distance of closest approach of the two adiabatic states.

I. INTRODUCTION

In Paper I of this series,[1] the adiabatic-state expansion method for atomic scattering and rearrangement collisions was critically examined. Several difficulties and ambiguities for rearrangement collisions were resolved. It was then shown that the use of the eikonal approximation to describe the motion of the atoms or ions or both permits the coupled equations of the adiabatic-state expansion method to be reduced to one-dimensional equations defined along classical trajectories. Several practical techniques for evaluating wave functions and Green's functions in the eikonal approximation were introduced in Paper II.[2] A variational technique based on the "principle of least action" was also developed in Paper II for the calculation of the trajectory. Numerical illustrations of these various techniques were carried out for the (H^+, H) and (He^+, He) collision systems in both the classical limit and the nonclassical regime of the eikonal approximation.[2,3] In all these applications, we were dealing essentially with potential-scattering problems. In the present paper we shall consider the problem of quasiadiabatic transitions in the multistate eikonal approximation.

The eikonal approximation will be valid if (in the notation of Paper I)

$$\eta_3 \equiv \hbar/pa_0 \ll 1 , \tag{1.1}$$

where p is the relative momentum of the colliding particles. Our approximation scheme is expected to converge rapidly if the adiabatic criterion is met:

$$\eta_2 = v/(e^2/\hbar) \ll 1 . \tag{1.2}$$

Let E be the initial kinetic energy (in a.u.) of the colliding particles in the c.m. system. We shall assume conditions (1.1) and (1.2) and, further, that

$$E \gg 1 , \tag{1.3}$$

which permits us (see Paper II) to calculate the eikonal with the approximation that the trajectories lie along straight lines. When condition (1.3) is met, the eikonal criterion [Eq. (1.1)] will always be satisfied.

In the adiabatic-state expansion method, the state function ψ_a^+ is represented by the expansion [see Eqs. (I2.14) and (I3.20)]

$$\psi_a^+ = \sum_\beta \varphi_\beta \Psi_\beta(R) , \tag{1.4}$$

with $\Psi_\beta(R)$ satisfying the coupled equations [see Eqs. (I2.18) and (I3.45)]

$$\Psi_\alpha = \delta_{\alpha 0}\Psi^+_{c0\vec{p}} + (E + i\eta - K - W_\alpha - \mathcal{V}_\alpha)^{-1} \sum_{\beta\neq\alpha} J_{\alpha\beta}\Psi_\beta , \tag{1.5}$$

where $W_\alpha + \mathcal{V}_\alpha$ are the eigenvalues of the adiabatic states φ_α, K is the appropriate kinetic energy operator of the colliding system in the c.m. system, and $J_{\alpha\beta}$ are the appropriately modified nonadiabatic interactions [see Eqs. (I2.16) and [I3.28)]. In Eq. (1.5) we have labeled the initial state as $\alpha = 0$ with incident relative momentum $\vec{p}$. Thus, the coherent state $\Psi^+_{c0\vec{p}}$ represents elastic scattering. The scattering matrix, for a final state α and relative momentum $\vec{k}$ is

$$\langle \alpha, \vec{k}| T|0, \vec{p}\rangle = \delta_{\alpha 0}(\lambda_k, U_0\Psi^+_{c0\vec{p}}) + \left(\Psi^-_{c\alpha\vec{k}}, \sum_{\beta\neq\alpha} J_{\alpha\beta}\Psi_\beta\right) . \tag{1.6}$$

We shall make use of the techniques developed in Paper II for evaluating wave functions and Green's functions in the reduction of the transition matrix elements. In Sec. II the matrix elements for quasiadiabatic transitions are reduced in the multistate eikonal approximation to a form that allows straightforward computations. We then consider the application of the multistate eikonal approximation in subsequent sections.

In Sec. III, a model (He^+, H) collision system is constructed based on the adiabatic HeH^+ states recently calculated by Michels.[4] The (He^+, H) model is constructed to provide a reasonably realistic representation of the $2p$-excitation process

$$He^+(1s) + H(1s) \rightarrow He^+(1s) + H(2p) . \tag{1.7}$$

In this (He^+, H) model, we have included six adiabatic molecular states. The nonadiabatic interactions between these adiabatic states are represented in this model by semiempirical formulas obtained from the exact asymptotic expressions of the nonadiabatic interactions.

A detailed investigation of quasiadiabatic transitions is carried out in Sec. IV in the eikonal Born approximation. In this investigation we have studied the qualitative features of the nonadiabatic effects as functions of the position and distance of closest approach of the two adiabatic states. The saddle-point approximation for the evaluation of the path integral[5] is then investigated and compared with the corresponding numerical results. The error resulting from the eikonal Born approximation is examined in the two-state eikonal approximation in which the back-and-forth coupling between the two states is explicitly accounted for.

The application of the multistate eikonal approximation to the $2p$ excitation of H atoms by He^+ ion impact is then carried out in Sec. V. We have calculated both the partial and total excitation cross sections as well as the polarization of the light emitted by the excited H atoms. Our results compare well with recent experimental measurements.[6] The importance of final-state interactions[7] is dramatically illustrated by the $2p$-excitation process of Eq. (1.7). A brief account of this work has appeared elsewhere.[8]

II. MULTICHANNEL EIKONAL APPROXIMATION

In this section, we consider the evaluation of the scattering matrix $\langle \alpha, \vec{k}| T|0, \vec{p}\rangle$ given by Eq. (1.6) for multichannel quasiadiabatic atomic processes. We shall consider first the simple eikonal Born approximation. This corresponds to the well-known Born approximation in which the coupling of other participating states is neglected. The eikonal Born approximation, however, improves the usual Born approximation by providing a more careful analysis of the phase relations between the two states. After deriving the eikonal Born approximation, we then investigate the coupling of participating states. In the multistate eikonal approximations, a set of coupled first-order differential equations is then derived for the eikonal amplitudes as well as the transition amplitudes. The cross section for the quasiadiabatic transitions can then be calculated in terms of the solutions of the coupled equations for the amplitudes.

A. Eikonal Born Approximation

The Born approximation to Eqs. (1.5) and (1.6) gives us the scattering matrix

$$T^B_{\alpha 0} \equiv (\Psi^-_{c\alpha\vec{k}}, J_{\alpha 0}(\vec{R}, -i\nabla)\Psi^+_{c0\vec{p}}) . \tag{2.1}$$

The matrix elements may be reduced to path integrals in the eikonal approximation. We have for the coherent state $\Psi^\pm_{c0\vec{p}}$ and the modified nonadiabatic interaction $J_{\alpha 0}(\vec{R}, -i\nabla)$ [see Eq. (I3.28)] the forms

$$\Psi^+_{c\alpha\vec{k}}(\vec{R}) = (2\pi)^{-3/2} A_\alpha(\vec{R}) e^{i S^+_k(\vec{R})} , \tag{2.2}$$

$$J_{\alpha 0}(\vec{R}, -i\nabla) \cong J_{\alpha 0}(\vec{R}, \vec{K}(\vec{R})) \equiv J_{\alpha 0}(\vec{R}) . \tag{2.3}$$

The matrix elements in the eikonal Born approximation then take the form

$$T^B_{\alpha 0} = (2\pi)^{-3} \int d^3R\, A_\alpha(\vec{R}) A_0(\vec{R}) J_{\alpha 0}(\vec{R})\, e^{i[S^+_{\vec{p}}(\vec{R}) - S^-_{\vec{k}}(\vec{R})]} . \tag{2.4}$$

The eikonals $S^\pm(\vec{R})$ have been evaluated in Paper II.

We shall use a coordinate system with the z axis parallel to $\vec{p}$. In this coordinate system, we shall suppose that $J_{\alpha 0}$ has cylindrical symmetry with the form

$$J_{\alpha 0}(\vec{R}) = J_{\alpha 0}(z, b) , \tag{2.5}$$

where b is the distance of a point $\vec{R}$ from the z axis, i.e., the impact parameter. The path integrals then take the form, to relative order $|\theta_c|$,

$$T^B_{\alpha 0} = (2\pi)^{-3} \int \rho\, d\rho\, d\varphi\, dz\, J_{\alpha 0}(z, b)\, e^{i[S^+_{\vec{p}}(\vec{R}) - S^-_{\vec{k}}(\vec{R})]}, \tag{2.6}$$

where we have taken $A(\vec{R}) = 1$ (which is valid to relative order $|\theta_c|$). From Eqs. (II3.14), we have for the eikonal

$$S^+_{\vec{p}}(\vec{R}) = p\bar{z}\sec\beta - pb\tan\beta + \Phi^+_0(\bar{z}, b), \tag{2.7}$$

$$S^-_{\vec{k}}(\vec{R}) = k\bar{z}\sec\beta + kb\tan\beta + \Phi^-_\alpha(\bar{z}, b), \tag{2.8}$$

with

$$\Phi^+_0(\bar{z}, b) = -p\int_{-\infty}^{\bar{z}} \{\tfrac{1}{2}[\beta^2 - \beta^2(\bar{z}')] + U_0(\vec{R})\}\, d\bar{z}', \tag{2.9}$$

$$\Phi^-_\alpha(\bar{z}, b) = k\int_{\bar{z}}^{\infty} \{\tfrac{1}{2}[\beta^2 - \beta^2(\bar{z}')] + U_\alpha(\vec{R})\}\, d\bar{z}', \tag{2.10}$$

$$\beta = \tfrac{1}{2}\theta_c = \lim_{\bar{z}\to\infty} \beta(\bar{z}), \tag{2.11}$$

$$U_0(\vec{R}) = 1 - [1 - \mathcal{V}_0(R)/\epsilon_p]^{1/2}, \tag{2.12}$$

where $\beta(z)$ and $\mathcal{V}(\vec{R})$ are defined by Eqs. (II2.2) and (I2.9), respectively. The coordinate $\bar{z}$, which was defined in Fig. 2 of Paper II, is related to z by a plane rotation through an angle β.

We shall use the straight-line approximation for the evaluation of the eikonal. This is valid when [see Eq. (II1.22)]

$$\eta_{es} = (920\, A_{\rm eff}/E^3)^{1/2} \ll 1, \tag{2.13}$$

where $A_{\rm eff}$ is the value of the reduced mass M_r expressed in units of the proton mass. We then have

$$S^+_{\vec{p}} - S^-_{\vec{k}} = (\vec{p} - \vec{k}_{\rm in})\cdot\vec{R} - kb\theta'_c + \Delta\Phi_{\alpha 0}(\bar{z}, b), \quad z < 0 \tag{2.14a}$$

$$= (\vec{p}_0 - \vec{k})\cdot\vec{R} - pb\theta_c + \Delta\Phi_{\alpha 0}(\bar{z}, b), \quad z > 0 \tag{2.14b}$$

with

$$\Delta\Phi_{\alpha 0}(\bar{z}, b) \equiv -p\int_{-\infty}^{\bar{z}} U_0(R_0)\, d\bar{z}' - k\int_{\bar{z}}^{\infty} U_\alpha(R_0)\, d\bar{z}', \tag{2.15}$$

$$R_0 = (\bar{z}^2 + b^2)^{1/2}, \tag{2.16}$$

where $\vec{p}_0$ and $\vec{k}_{\rm in}$ are the asymptotic relative momenta in the post and prior regions, respectively.

Let $\vec{k}$ lie in the xz plane and $\vec{p}_0$ be radial. It then follows that

$$\begin{aligned}
\vec{k}_{\rm in}\cdot\vec{R} &= k\cos\theta'_c[z\cos\theta + \rho\sin\theta\cos\varphi] \\
&\quad - k\sin\theta'_c[\rho - z\cos\theta\sin\theta\cos\varphi], \\
\vec{p}\cdot\vec{R} &= pz, \\
\vec{p}_0\cdot\vec{R} &= p\cos\theta_c z + p\rho\sin\theta_c, \\
\vec{k}\cdot\vec{R} &= k\cos\theta\, z + k\rho\sin\theta\cos\varphi,
\end{aligned} \tag{2.17}$$

where θ is the scattering angle, $\theta = \cos^{-1}(\hat{p}\cdot\hat{k})$. To relative order $|\theta_c|$, we then have for all values of z

$$S^+_{\vec{p}} - S^-_{\vec{k}} \cong (p - k)z - k\rho\sin\theta\cos\varphi + \Delta\Phi_{\alpha 0}(\bar{z}, b). \tag{2.18}$$

After integrating over φ, the path integrals given by Eq. (2.6) reduce to the form

$$T^B_{\alpha 0} = (2\pi)^{-2}\int_0^\infty b\, db\, J_0(kb\sin\theta) \times \int_{-\infty}^{\infty} d\bar{z}\, J_{\alpha 0}(z, b)\, e^{i[(p-k)z + \Delta\Phi_{\alpha 0}(\bar{z}, b)]}, \tag{2.19}$$

where we have made use of the approximation

$$\rho\, d\rho\, dz \cong b\, d\, b\, d\bar{z}, \tag{2.20}$$

which is valid to relative order $|\theta_c|$.

The identity

$$\Delta\Phi_{\alpha 0}(\bar{z}, b) = \tfrac{1}{2}\Phi_{\alpha 0}(b) + \delta\Phi_{\alpha 0}(\bar{z}, b), \tag{2.21}$$

with

$$\Phi_{\alpha 0}(b) \equiv \Phi_\alpha(b) + \Phi_0(b) = -\int_{-\infty}^{\infty} [kU_\alpha(R_0) + pU_0(R_0)]\, dz \tag{2.22}$$

and

$$\delta\Phi_{\alpha 0}(\bar{z}, b) = -\int_0^{\bar{z}} [pU_0 - kU_\alpha]\, d\bar{z}', \tag{2.23}$$

permits Eq. (2.19) to be rewritten as

$$T^B_{\alpha 0} = (2\pi)^{-2}\int_0^\infty b\, db\, J_0(kb\sin\theta)\, Q^B_{\alpha 0}(b)\, e^{(i/2)\Phi_{\alpha 0}(b)}, \tag{2.24}$$

with

$$Q^B_{\alpha 0}(b) = \int_{-\infty}^{\infty} d\bar{z}\, J_{\alpha 0}(z, b)\, e^{i[z(p-k) + \delta\Phi_{\alpha 0}(\bar{z}, b)]}. \tag{2.25}$$

The local phase difference $\delta\Phi_{\alpha 0}(\bar{z}, b)$ can be rewritten as

$$\delta\Phi_{\alpha 0}(\bar{z}, b) = \int_0^{\bar{z}} \left(\frac{1}{v_k}\mathcal{V}_\alpha - \frac{1}{v_p}\mathcal{V}_0\right) dz', \tag{2.26}$$

where we have assumed that $\mathcal{V}_\alpha$ and $\mathcal{V}_0$ are small in comparison with the total energy E.[9] The transition amplitude given by Eq. (2.24) may be solved by the stationary-phase approximation in the classical limit. This is shown in Appendix A.

The differential cross section in the eikonal Born approximation may be obtained from $T^B_{\alpha 0}$:

$$\frac{d\sigma^B}{d\Omega} = (2\pi)^4 M_r^2 \frac{v_k}{v_p} |T^B_{\alpha 0}|^2. \tag{2.27}$$

The total cross section

$$\sigma = \int \frac{d\sigma}{d\Omega}\, d\Omega \tag{2.28}$$

can then be obtained from Eq. (2.27) in the simple form

$$\sigma^B \cong \frac{2\pi}{v_k^2}\int_0^\infty b\, db\, |Q^B_{\alpha 0}(b)|^2, \tag{2.29}$$

where we have made use of the approximation given by Eq. (II5.23).

B. Multistate Eikonal Approximation

In atomic collisions, a number of adiabatic states which are closely spaced would participate in the

interaction simultaneously. To provide an adequate description of such collisions, one must account for the dynamic coupling of these states. For such collisions, Eq. (1.5) may be solved directly. We consider the case that only a finite number of adiabatic states α need be included and that the energy E is large compared with the spacings of these states.

We rewrite Eq. (1.5) as

$$\Psi_\alpha = \delta_{\alpha 0}\Psi^+_{c\vec{0}} + \sum_{\beta(\neq\alpha)} G_\alpha J_{\alpha\beta}\Psi_\beta \ , \tag{2.30}$$

where in our eikonal approximation the Green's function takes the form

$$G_\alpha(\vec{R}, \vec{R}') = -(M_r/2\pi)\,|\vec{R}-\vec{R}'|^{-1}\, e^{iS_\alpha(\vec{R},\vec{R}')} \ . \tag{2.31}$$

Here

$$S_\alpha(\vec{R}, \vec{R}') = \int_{\vec{R}'}^{\vec{R}} \kappa_\alpha(\bar{R})\, ds \ , \tag{2.32}$$

with

$$\kappa_\alpha = [2M_r(E - W_\alpha - \mathcal{V}_\alpha)]^{1/2} \ , \tag{2.33}$$

and the path of integration runs over that trajectory which passes through $\vec{R}'$ and $\vec{R}$.

We attempt to solve Eq. (2.30) with the ansatz

$$\Psi_\beta(\vec{R}') = (2\pi)^{-3/2}\gamma_\beta(\vec{R}')\, e^{iS_\beta(\vec{R}')} \ , \tag{2.34}$$

where it is supposed that the eikonal amplitude γ_β is a relatively slowly varying function of position and $S_\beta(\vec{R})$ is the eikonal function

$$S_\beta(\vec{R}) = \int^{\vec{R}} \kappa_\beta\, ds \ . \tag{2.35}$$

Here, in the straight-line approximation, the path integral is taken parallel to $\vec{p}$ and

$$\lim_{\vec{p}\cdot\vec{R}\to-\infty} S_\beta(\vec{R}) = [2M_r(E - W_\beta)]^{1/2}\,\hat{p}\cdot\vec{R} \ . \tag{2.36}$$

(See Secs. II and III of Paper II for a discussion of boundary conditions for the eikonal.)

Now, let us define

$$\vec{r} = \vec{R}' - \vec{R} \tag{2.37}$$

and write

$$S_\alpha(\vec{R}, \vec{R}') \cong \kappa_\alpha(R) r \ , \tag{2.38}$$

$$S_\beta(\vec{R}') \cong \vec{\kappa}_\beta(\vec{R})\cdot\vec{r} + S_\beta(\vec{R}) \ , \tag{2.39}$$

where $\vec{\kappa}_\beta = \kappa_\beta\hat{p}$. When Eqs. (2.31), (2.34), and (2.37)–(2.39) are used, the quantity $G_\alpha J_{\alpha\beta}\Psi_\beta$ takes the form

$$G_\alpha J_{\alpha\beta}\Psi_\beta = -\frac{M_r}{(2\pi)^{5/2}}\, e^{iS_\beta(\vec{R})}\int_0^\infty r\, dr\, e^{i\kappa_\alpha(R)r} I_{\alpha\beta}(\vec{R}, r) \ , \tag{2.40}$$

with

$$I_{\alpha\beta}(\vec{R}, r) = \int d\hat{r}\, e^{i\vec{\kappa}_\beta(\vec{R})\cdot\vec{r}} J_{\alpha\beta}(\vec{R}+\vec{r})\,\gamma_\beta(\vec{R}+\vec{r}) \ , \tag{2.41}$$

where the angular integral can be approximately evaluated to give

$$I_{\alpha\beta}(\vec{R}, r) \cong (2\pi/i\kappa_\beta r)\,[e^{i\kappa_\beta r} J_{\alpha\beta}(\vec{R}+\hat{p}r)\,\gamma_\beta(\vec{R}+\hat{p}r) - e^{-i\kappa_\beta r} J_{\alpha\beta}(\vec{R}-\hat{p}r)\,\gamma_\beta(\vec{R}-\hat{p}r)] \ . \tag{2.42}$$

Then for $\kappa_\alpha r \gg 1$, the conventional asymptotic evaluation gives us

$$G_\alpha J_{\alpha\beta}\Psi_\beta \cong \frac{M_r e^{iS_\beta(\vec{R})}}{i\kappa_\beta(2\pi)^{3/2}}\int dr\, J_{\alpha\beta}(\vec{R}-\hat{p}r)\,\gamma_\beta(\vec{R}-\hat{p}r) \times e^{i[\kappa_\alpha(R)-\kappa_\beta(R)]r} \ . \tag{2.43}$$

Because of the assumed cylindrical symmetry of $J_{\alpha\beta}$, we have

$$J_{\alpha\beta}(\vec{R}-\hat{p}r) = J_{\alpha\beta}(z-r, b) \ , \tag{2.44}$$

$$\gamma_\beta(\vec{R}-\hat{p}r) = \gamma_\beta(z-r, b) \ . \tag{2.45}$$

Let us define

$$z' = z - r \ ; \tag{2.46}$$

we then have

$$[\kappa_\alpha(R) - \kappa_\beta(R)]r \cong S_\alpha(z, b) - S_\beta(z, b) - [S_\alpha(z', b) - S_\beta(z', b)] \ . \tag{2.47}$$

Taking this together with Eq. (2.43), we write, finally,

$$\Psi_\alpha(\vec{R}) = \delta_{\alpha 0}\Psi^+_{c\vec{0}}(\vec{R}) - \sum_{\beta\neq\alpha} \frac{ie^{iS_\alpha(z,b)}}{v_\beta(2\pi)^{3/2}} \times\int_{-\infty}^{z} dz'\, J_{\alpha\beta}(z', b)\,\gamma_\beta(z', b)\, e^{-i\phi_{\alpha\beta}(z', b)} \ . \tag{2.48}$$

Here we have set

$$v_\beta = \kappa_\beta/M_r \cong v_{\rm rel} \tag{2.49}$$

and

$$\phi_{\alpha\beta}(z', b) \equiv S_\alpha(\vec{R}') - S_\beta(\vec{R}') \ . \tag{2.50}$$

Equation (2.48) can be further simplified. Substitution of Eq. (2.2) for $\Psi^+_{c\alpha\vec{0}}(\vec{R})$ and Eq. (2.34) for $\Psi_\alpha(\vec{R})$ into Eq. (2.48) yields the set of coupled equations for the eikonal amplitudes γ_α:

$$\gamma_\alpha(z, b) = \delta_{\alpha 0} - i\sum_{\beta\neq\alpha}^{N}\int_{-\infty}^{z} dz'\,\Lambda_{\alpha\beta}(z', b)\,\gamma_\beta(z', b) \tag{2.51}$$

or

$$\frac{d\gamma_\alpha(z, b)}{dz} = -i\sum_{\beta\neq\alpha}^{N}\Lambda_{\alpha\beta}(z, b)\,\gamma_\beta(z, b) \ , \tag{2.52}$$

with

$$\Lambda_{\alpha\beta}(z, b) \equiv v_\beta^{-1} J_{\alpha\beta}(z, b)\, e^{-i\phi_{\alpha\beta}(z,b)} \ . \tag{2.53}$$

The boundary condition for the eikonal amplitudes is

$$\gamma_0(z, b)\to 1 \ \text{ as } z\to-\infty \ , \qquad \gamma_\alpha(z, b)\to 0 \ \text{ as } z\to-\infty \text{ for } \alpha\neq 0 \ , \tag{2.54}$$

which merely states the fact that in the asymptotic prior region the scattering system is in the $|0\vec{p}\rangle$ state.

The scattering matrix $\langle \alpha\vec{k}\,|\,T\,|\,0\vec{p}\,\rangle$ given by Eq. (1.6) can also be evaluated in the multistate eikonal approximation. Considering the case $\alpha \neq 0$, we have

$$T_{\alpha 0}^{(N)} \equiv (2\pi)^{-3} \sum_{\beta \neq \alpha}^{N} \int d^3R\, A_\alpha(\vec{R})\, J_{\alpha\beta}(\vec{R})\, \gamma_\beta(\vec{R}) \times e^{i[S_\beta(\vec{R}) - S_{\vec{k}}(\vec{R})]} . \quad (2.55)$$

This path integral can be evaluated just as before for Eq. (2.4). We obtain

$$T_{\alpha 0}^{(N)} = (2\pi)^{-2} \int_0^\infty b\, db\, J_0(kb\sin\theta)\, Q_{\alpha 0}^{(N)}(b)\, e^{(i/2)\Phi_{\alpha 0}(b)} , \quad (2.56)$$

with

$$Q_{\alpha 0}^{(N)}(b) = e^{(i/2)[\Phi_\alpha(b) - \Phi_0(b)]} \sum_{\beta \neq \alpha}^{N} \int_{-\infty}^{\infty} dz'\, J_{\alpha\beta}(z', b) \times e^{-i\phi_{\alpha\beta}(z', b)}\, \gamma_\beta(z', b) , \quad (2.57)$$

where the $\phi_{\alpha\beta}(z', b)$ are given by Eq. (2.50). For the case with $\beta = 0$ we have

$$-\phi_{\alpha 0}(z, b) = z(p - k) + \delta\Phi_{\alpha 0}(z, b) + \tfrac{1}{2}[\Phi_0(b) - \Phi_\alpha(b)] . \quad (2.58)$$

It is then clear that Eqs. (2.56) and (2.57) reduce to Eqs. (2.24) and (2.25) in the eikonal Born approximation by setting $\gamma_0 = 1$. The total cross section can again be expressed in the approximate form given by Eq. (2.29) with $Q_{\alpha 0}^{B}(b)$ replaced by $Q_{\alpha 0}^{(N)}(b)$.

It is, however, convenient to introduce the modified equations obtained from Eq. (2.57):

$$Q_\alpha(z, b) = \sum_{\beta \neq \alpha}^{N} \int_{-\infty}^{z} dz'\, \Lambda_{\alpha\beta}(z', b)\, \gamma_\beta(z', b) , \quad (2.59)$$

with

$$Q_\alpha(z, b) \equiv v_{\rm rel}^{-1}\, Q_{\alpha 0}^{(N)}(z, b)\, e^{(i/2)[\Phi_0(b) - \Phi_\alpha(b)]} . \quad (2.60)$$

From the comparison of Eq. (2.59) with Eq. (2.51), it is clear that

$$\gamma_\alpha(z, b) = \delta_{\alpha 0} - iQ_\alpha(z, b) . \quad (2.61)$$

Consequently

$$\frac{dQ_\alpha(z, b)}{dz} = \sum_{\beta \neq \alpha}^{N} \Lambda_{\alpha\beta}(z, b)\, \gamma_\beta(z, b) = \Lambda_{\alpha 0}(1 - \delta_{\alpha 0}) - i \sum_{\beta \neq \alpha}^{N} \Lambda_{\alpha\beta} Q_\beta . \quad (2.62)$$

It is apparent that $Q_\alpha(z, b)$ in the limit $z \to \infty$ is the transition amplitude. In terms of $Q_\alpha(\infty, b)$, the total cross section takes the form

$$\sigma_{\alpha 0} \cong 2\pi \int_0^\infty b\, db\, |\, Q_\alpha(\infty, b)|^2 . \quad (2.63)$$

III. MODEL (He^+, H) COLLISION SYSTEM

In this section, we construct a reasonably realistic multichannel model system for quasiadiabatic collisions. In Sec. IV we apply our eikonal Born approximation to this model system and investigate the qualitative features of the quasiadiabatic (diabatic) transitions. In Sec. V, an application of our multistate eikonal approximation to this model system is carried out in order to investigate the final-state interactions in a quasiadiabatic excitation process. With these applications in mind, we construct our model to represent the (He^+, H) system. This is the simplest two-electron heteronuclear molecular system. In addition, experimental measurement of the

$$He^+(1s) + H(1s) \to He^+(1s) + H(2p) \quad (3.1)$$

$2p$-excitation process has recently become available.[6]

A. Adiabatic He H^+ States φ_a

The nonrelativistic Hamiltonian for the (He^+, H) system can be written as

$$H = -(1/2M_r)\nabla_{R_1}{}^2 + h_a + 2e^2/R , \quad (3.2)$$

with

$$h_a = \left(K_1 - \frac{e^2}{|\vec{r}_1|} - \frac{2e^2}{|\vec{R}_1 + \vec{r}_1|}\right) + \left(K_2 - \frac{2e^2}{|\vec{r}_2|} - \frac{e^2}{|\vec{R}_1 - \vec{r}_2|}\right) + \frac{e^2}{|\vec{R}_1 + \vec{r}_1 - \vec{r}_2|} , \quad (3.3)$$

where K_1 and K_2 are kinetic-energy operators of the two electrons labeled as 1 and 2. The adiabatic states are defined to be the eigenstates of the adiabatic Hamiltonian h_a:

$$h_a \varphi_\alpha = w_\alpha(\vec{R}_1)\varphi_\alpha . \quad (3.4)$$

The eigenvalues $w_\alpha(\vec{R})$ give rise to the adiabatic potential $v_\alpha(R)$

$$v_\alpha(\vec{R}_1) \equiv w_\alpha(\vec{R}_1) - \lim_{\vec{R}_1 \to \infty} w_\alpha \quad (3.5)$$

for the He^+-H interaction.

For a reasonable description of the $2p$-excitation process of Eq. (3.1), we need to consider a number of such adiabatic states. For the $2p$ excitation in the singlet spin multiplicity, we take into consideration the $A\,^1\Sigma$, $C\,^1\Pi$, and $E\,^1\Sigma$ adiabatic HeH^+ states. For the triplet $2p$ excitation, we take the $a\,^3\Sigma$, $e\,^3\Pi$, and $f\,^3\Sigma$ adiabatic HeH^+ states into consideration. The correlation of these adiabatic molecular electronic states with the separated as well as the united atomic states is summarized in Table I.

These adiabatic HeH^+ states have recently been calculated by Michels for several values of the internuclear separation.[4] Using these calculated values, we have constructed a model set of adiabatic HeH^+ interaction potentials by extrapolating the calculated HeH^+ molecular states to their appropriate Li^+ united atomic states. This set of model adiabatic HeH^+ potentials are shown in Figs. 1 and 2 with and without the $2/R$ nuclear interaction, re-

TABLE I. Correlations of atomic and molecular states for HeH^+.

United atom ($R=0$)		Molecular state	Separated atoms ($R=\infty$)	
$Li^+[^1S(1s2s)]$	−5.047 15	$A\,^1\Sigma$	$He^+[^2S(1s)]+H[^2S(1s)]$	−2.500
$Li^+[^1P(1s3p_\pi)]$	−4.720 325	$C\,^1\Pi$	$He^+[^2S(1s)]+H[^2P(2p_\pi)]$	−2.125
$Li^+[^1D(1s3d_\sigma)]$	−4.722 2	$E\,^1\Sigma$	$He^+[^2S(1s)]+H[^2P)2p_0)]$	−2.125
$Li^+[^3S(1s2s)]$	−5.111 025	$a\,^3\Sigma$	$He^+[^2S(1s)]+H[^2S(1s)]$	−2.500
$Li^+[^3P(1s3p_\pi)]$	−4.730 573	$e\,^3\Pi$	$He^+[^2S(1s)]+H[^2P(2p_\pi)]$	−2.125
$Li^+[^3P(1s3p_\sigma)]$	−4.730 573	$f\,^3\Sigma$	$He^+[^2S(1s)]+H[^2P(2p_\sigma)]$	−2.125

spectively. Analytic fittings of these potentials are given in Appendix B.

In this six-state model we have included the coupling of channels arising from the asymptotically degenerate $2p_\sigma$ and $2p_\pi$ states. There are a number of channels also asymptotically degenerate or near degenerate with the $2p$ excitation channels which were not included in this model. For example, we have neglected the coupling with the $2s$ excitation channel as well as the electron-transfer rearrangement channels in which the He atom is formed in the $(1s)(2s)$ and $(1s)(2p)$ atomic states. As a first example for the application of the multichannel eikonal approximation derived in Sec. II, we shall neglect the latter channels and confine our treatment in the simple six-state model which should give a reasonable description of the $2p$-excitation process.

B. Nonadiabtic Interaction $J_{\alpha\beta}$

In addition to the adiabatic HeH^+ states, we require in the model the interaction between adiabatic states. Such a nonadiabatic interaction is essentially given by the Born-Oppenheimer (BO) matrix elements [see Eq. (I3.22)]

$$\Delta_{\alpha\beta}=-\frac{1}{2M}[(\varphi_\alpha,\nabla_{R_1}{}^2\varphi_\beta)+2(\varphi_\alpha\nabla_{R_1}\varphi_\beta)\cdot\nabla_{R_1}]\,. \tag{3.6}$$

To account for rearrangement collisions, we write this nonadiabatic interaction $J_{\alpha\beta}$ as

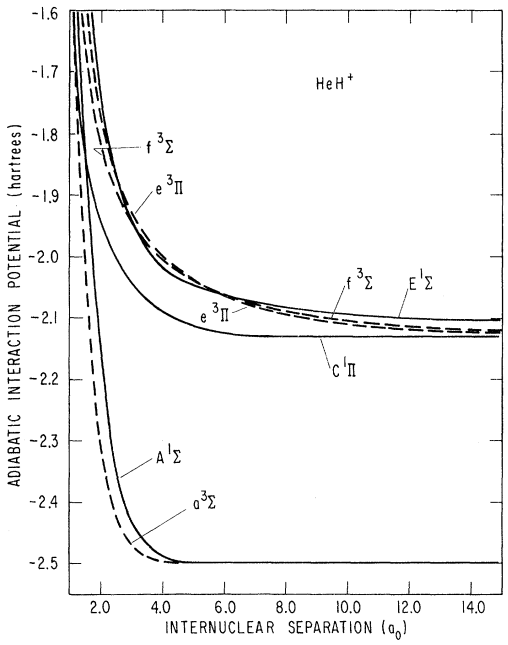

FIG. 1. Adiabatic interaction potentials for He^+ and H. These potentials which are relevant for the $2p$ excitation of H atoms by He^+ ion impact are constructed from the recent calculation of Michels (Ref. 4).

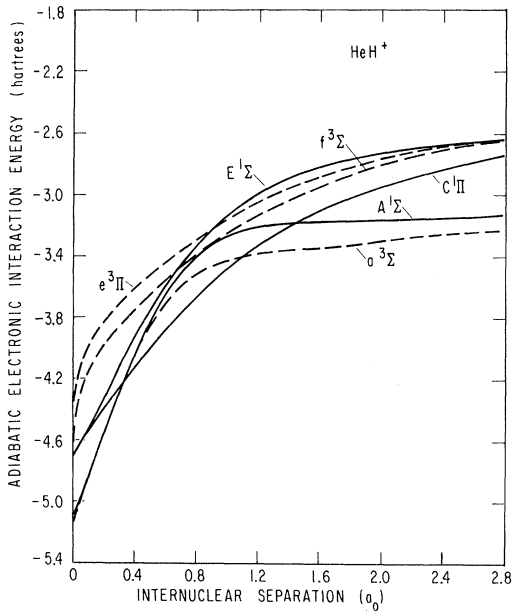

FIG. 2. Electronic energies of adiabatic HeH^+ states. These states which participate in the $2p$ excitation of H atoms by He^+ ion impact are constructed from the recent calculation of Michels (Ref. 4) with particular attention to the united atom limit.

$$J_{\alpha\beta} = \Delta_{\alpha\beta} - \lim_{R_1 \to \infty} \Delta_{\alpha\beta} \tag{3.7}$$

(for a detailed discussion, we refer to Sec. III of Paper I). This guarantees that $J_{\alpha\beta} = 0$ in the limit $R_1 \to \infty$.

In the eikonal approximation, the nonadiabatic interaction may be written as [see Eq. (2.3)]

$$J_{\alpha\beta}(\vec{R}_1) = -\frac{i\vec{k}}{M_r} \cdot (\varphi_\alpha, \nabla_{R_1}\varphi_\beta) - \frac{1}{2M_r}(\varphi_\alpha, \nabla_{R_1}{}^2\varphi_\beta) . \tag{3.8}$$

The identity

$$(w_\alpha - w_\beta)(\varphi_\alpha, \nabla_{R_1}\varphi_\beta) = -(\varphi_\alpha, \nabla_{R_1} h_a \varphi_\beta) \tag{3.9}$$

permits us to rewrite Eq. (3.8) as

$$J_{\alpha\beta}(\vec{R}_1) = \frac{i\vec{k} \cdot (\varphi_\alpha, (\nabla_{R_1} h_a)\varphi_\beta)}{M_r(w_\alpha - w_\beta)} - \frac{1}{2M_r}(\varphi_\alpha, \nabla_{R_1}{}^2\varphi_\beta) . \tag{3.10}$$

The second term on the right-hand side of Eq. (3.10) is comparatively much smaller and will be neglected in the following considerations. It is understood that if $\Delta_{\alpha\beta} \neq 0$ in the limit $R_1 \to \infty$, $J_{\alpha\beta}$ should be redefined according to Eq. (3.7).

The gradient of the adiabatic Hamiltonian for the (He^+, H) system may be written as

$$(\nabla_{R_1} h_a) = \nabla_{R_1}\left(\frac{e^2}{|\vec{R}_1 + \vec{r}_1 - \vec{r}_2|} - \frac{2e^2}{|\vec{R}_1 + \vec{r}_1|} - \frac{e^2}{|\vec{R}_1 - \vec{r}_2|}\right) , \tag{3.11}$$

with

$$\nabla_{R_1}\left(\frac{e^2}{|\vec{R}_1 + \vec{r}_1 - \vec{r}_2|}\right) = -e^2 \frac{\vec{R}_1 + \vec{r}_1 - \vec{r}_2}{|\vec{R}_1 + \vec{r}_1 - \vec{r}_2|^3} , \tag{3.12}$$

$$\nabla_{R_1}\left(-\frac{2e^2}{|\vec{R}_1 + \vec{r}_1|}\right) = 2e^2 \frac{\vec{R}_1 + \vec{r}_1}{|\vec{R}_1 + \vec{r}_1|^3} , \tag{3.13}$$

$$\nabla_{R_1}\left(-\frac{e^2}{|\vec{R}_1 - \vec{r}_2|}\right) = e^2 \frac{\vec{R}_1 - \vec{r}_2}{|\vec{R}_1 - \vec{r}_2|^3} . \tag{3.14}$$

The BO matrix elements in Eq. (3.10) can then be computed if the adiabatic states are available. It is rather unfortunate that in the past such BO matrix elements were not calculated when the adiabatic states were optimized in the determination of the energy eigenvalues. The inclusion of BO matrix elements will not greatly increase the computation. This is particularly true in the straight-line approximation, for which we have, for example,

$$\begin{aligned}(\varphi_\alpha(\vec{r}, \vec{R}_1), \nabla_{R_1}\varphi_\beta(\vec{r}, \vec{R}_1)) &\cong \hat{z}(\varphi_\alpha(\vec{r}, b, z), (\partial/\partial z)\varphi_\beta(\vec{r}, b, z)) \\ &= (\hat{z}/\Delta z)[(\varphi_\alpha(\vec{r}, b, z), \varphi_\beta(\vec{r}, b, z + \Delta z)) - \delta_{\alpha\beta}] ,\end{aligned} \tag{3.15}$$

where we have taken $R_1 = (b^2 + z^2)^{1/2}$.

These matrix elements at large internuclear separations can be determined analytically using the separated atom approximation. It can be shown that, in the limit $R_1 \to \infty$, we have, for finite r_1 and r_2, the asymptotic expressions for the potential gradients [see Eq. (C1)]

$$\nabla_{R_1}\left(\frac{e^2}{|\vec{R}_1 + \vec{r}_1 - \vec{r}_2|}\right) \to -\frac{e^2\vec{R}_1}{R_1^3} - \frac{e^2}{R_1^3}\{(\vec{r}_1 - \vec{r}_2) - 3\hat{R}_1[\hat{R}_1 \cdot (\vec{r}_1 - \vec{r}_2)]\} , \tag{3.16}$$

$$\nabla_{R_1}\left(-\frac{2e^2}{|\vec{R}_1 + \vec{r}_1|}\right) \to \frac{2e^2\vec{R}_1}{R_1^3} + \frac{2e^2}{R_1^3}[\vec{r}_1 - 3\hat{R}_1(\hat{R}_1 \cdot \vec{r}_1)] , \tag{3.17}$$

$$\nabla_{R_1}\left(-\frac{e^2}{|\vec{R}_1 - \vec{r}_2|}\right) \to \frac{e^2\vec{R}_1}{R_1^3} - \frac{e^2}{R_1^3}[\vec{r}_2 - 3\hat{R}_1(\hat{R}_1 \cdot \vec{r}_2)] . \tag{3.18}$$

Consequently, we have

$$(\nabla_{R_1} h_a) = \frac{2e^2\vec{R}_1}{R_1^3} + \frac{e^2}{R_1^3}[\vec{r}_1 - 3\hat{R}_1(\hat{R} \cdot \vec{r}_1)] + O\left(\frac{1}{R^4}\right) . \tag{3.19}$$

In this asymptotic region, the adiabatic molecular states go over to the atomic states

$$\lim_{R_1 \to \infty} \varphi_\alpha = g_\alpha . \tag{3.20}$$

For the $2p$-excitation process of Eq. (3.1) including only the adiabatic states given in Table I, g_α are simply the proper antisymmetric product of He^+ and H atomic wave functions:

$$g_\alpha = \mathcal{A}[R_{1s}^{He^+}(r_2)\, Y_0^0(\hat{r}_2) R_{2p}^{H}(r_1)\, Y_1^m(\hat{r}_1)] , \tag{3.21}$$

$$g_0 = \mathcal{A}[R_{1s}^{He^+}(r_2)\, Y_0^0(\hat{r}_2) R_{1s}^{H}(r_1)\, Y_0^0(\hat{r}_1)] . \tag{3.22}$$

The nonadiabatic interaction between the initial and final states takes, in this asymptotic region, the form

$$\lim_{R_1 \to \infty} J_{\alpha 0}(1s \to 2p_{0,\pm 1}) = \frac{ie^2}{\Delta W_{\alpha 0}}\left(\frac{k}{M_r}\right)\frac{g(1s \to 2p_{0,\pm 1})}{R_1^3} , \tag{3.23}$$

with

$$\Delta W_{\alpha 0} = \lim_{R_1 \to \infty}[w_\alpha(R_1) - w_0(R_1)] , \tag{3.24}$$

$$g(1s \to 2p_{0,\pm 1}) = (R_{2p}^{H}(r_1) Y_1^m(\hat{r}_1), \times \hat{k} \cdot [\vec{r}_1 - 3\hat{R}_1 \quad (\hat{R}_1 \cdot \vec{r}_1)] R_{1s}^{H}(r_1) Y_0^0(\hat{r}_1)) , \tag{3.25}$$

where we have taken the local tangent $\hat{k}$ to be in the direction of $\hat{k}$ parallel to the z axis. Now, let $\hat{R}_1$ lie in the xz plane and $\hat{k} \cdot \hat{R}_1 = \cos\gamma$. We then have

$$\hat{k} \cdot [\vec{r}_1 - 3\hat{R}_1 \quad (\hat{R}_1 \cdot \vec{r}_1)] = z(1 - 3\cos^2\gamma) - 3x\sin\gamma\cos\gamma . \tag{3.26}$$

Thus, we obtain

$$g(1s \to 2p_0) = (2^{15}/3^{10})^{1/2}(1 - 3\cos^2\gamma) , \tag{3.27}$$

$$g(1s \to 2p_\pm) = \pm(2^7/3^4)\sin\gamma\cos\gamma . \tag{3.28}$$

We also need the nonadiabatic interaction $J_{\alpha\beta}$ between the final states in the asymptotic region.

From parity considerations, it is clear that the corresponding matrix $g(2p_0 \to 2p_\pm)$ is zero. We must therefore consider the higher-order terms in Eq. (3.19). We then obtain (see Appendix C) the asymptotic expression for the nonadiabatic interaction between final states

$$\lim_{R_1 \to \infty} J_{\alpha\beta}(2p_0 \to 2p_{\pm 1}) = \frac{ie^2}{\Delta w_{\alpha\beta}} \left(\frac{k}{M_r}\right) \frac{g(2p_0 \to 2p_{\pm 1})}{R_1^4} , \tag{3.29}$$

with

$$g(2p_0 \to 2p_{\pm 1}) = (90/\sqrt{2}) \sin\gamma(\cos^2\gamma - \tfrac{1}{5}) . \tag{3.30}$$

This then completes the derivation of the nonadiabatic interactions in the asymptotic region.

In our model (He^+, H) system, we shall adopt semiempirical expressions for the nonadiabatic interaction obtained from the above asymptotic expressions upon replacing R_1 by $(R_1^2 + a^2)^{1/2}$. We have

$$J_{\sigma\sigma}(1s \to 2p_0) = \frac{ie^2 v_{\rm rel}\sqrt{2}}{\Delta W_{\alpha 0}} \left(\frac{2^8}{3^5}\right)\left(\frac{1}{(R_1^2 + a_\sigma^2)^{3/2}} - \frac{3z^2}{(R_1^2 + a_\sigma^2)^{5/2}}\right) , \tag{3.31}$$

$$J_{\pi\sigma}(1s \to 2p_{\pm 1}) = \pm \frac{ie^2 v_{\rm rel}}{\Delta W_{\alpha 0}} \left(\frac{2^7}{3^4}\right) \frac{bz}{(R_1^2 + a_\pi^2)^{5/2}} , \tag{3.32}$$

and

$$J_{\pi\sigma}(2p_0 \to 2p_{\pm 1}) = \frac{ie^2 v_{\rm rel}}{\Delta w_{\alpha 0}} \left(\frac{90}{\sqrt{2}}\right) \frac{b}{(R_1^2 + a_{\pi 2}^2)^2} \left(\frac{z^2}{R_1^2 + a_{\pi 1}^2} - \frac{1}{5}\right) , \tag{3.33}$$

where we have made use of the relations

$$\cos\gamma = z/R_1 , \quad \sin\gamma = b/R_1 . \tag{3.34}$$

The parameters $a_{|\lambda|}$ are to be determined semiempirically. We note that in Eqs. (3.31)–(3.33) we have labeled the nonadiabatic interactions by their corresponding momentum along the molecular axis.

IV. APPLICATION OF EIKONAL BORN APPROXIMATION

As we have already noted in Sec. III, from the spacing of the adiabatic states it is clear that a reasonable treatment of the $2p$ excitation in the (He^+, H) system requires at least the explicit consideration of the close couplings of those states given in Table I. Before engaging in such a calculation, we first examine the qualitative features of quasiadiabatic transitions in the eikonal Born approximation. A comparison of the eikonal Born approximation with the Glauber approximation as applied to the e-H excitations[10] is given elsewhere.[11]

To calculate the cross section for the quasiadiabatic transitions in the eikonal Born approximation, the quantity $Q^B_{\alpha 0}(b)$ given by Eq. (2.25) must be first determined. This can be done numerically using Eq. (2.23) [or Eq. (2.26)] for the local phase difference $\delta\Phi_{\alpha 0}(z, b)$ and Eqs. (3.29) and (3.30) for the $\sigma \to \sigma$ and $\sigma \to \pi$ nonadiabatic interactions, repectively. At high energies, $v_p \cong v_k = v_{\rm rel}$, and consequently $\delta\Phi_{\alpha 0}(z, b)$ is given by the potential difference $\Delta\mathcal{V}_{\alpha 0} = \mathcal{V}_\alpha - \mathcal{V}_0$

$$\delta\Phi_{\alpha 0}(\bar{z}, b) = (1/v_{\rm rel}) \int_0^{\bar{z}} \Delta\mathcal{V}_{\alpha 0}(\bar{z}', b)\, d\bar{z} . \tag{4.1}$$

A. Constant-Spacing Model

As a first example of the two-state eikonal approximation we consider the special case in which the potential difference is zero. In this case $\delta\Phi_{\alpha 0}$ is zero and $Q^B_{\alpha 0}(b)$ can be evaluated analytically. We have

$$Q^B_{\alpha 0}(b) = \int_{-\infty}^{\infty} dz\, J_{\alpha 0}(z, b)\, e^{-z(p-k)} . \tag{4.2}$$

The nonadiabatic interaction $J_{\alpha 0}$ is given by Eq. (3.31) for $\sigma \to \sigma$ transitions and by Eq. (3.32) for $\sigma \to \pi$ transitions. We have

$$Q^B_{\alpha 0}(b, \sigma \to \sigma) = \frac{ie^2 v_{\rm rel}}{\Delta W} \left(\frac{2^{9+1/2}}{3^5}\right) \int_0^\infty dz \cos(\zeta z) \times \left(\frac{3(b^2 + a_\sigma^2)}{(z^2 + b^2 + a_\sigma^2)^{5/2}} - \frac{2}{(z^2 + b^2 + a_\sigma^2)^{3/2}}\right) , \tag{4.3}$$

$$Q^B_{\alpha 0}(b, \sigma \to \pi) = \pm \frac{ie^2 v_{\rm rel}}{\Delta W} \left(\frac{2^8}{3^4}\right) \times \int_0^\infty dz \sin(\zeta z) \frac{bz}{(z^2 + b^2 + a_\pi^2)^{5/2}} , \tag{4.4}$$

with

$$\zeta \equiv (p - k) = \frac{\Delta W}{(p + k)/(2M_r)} \cong \frac{\Delta W}{v_{\rm rel}} , \tag{4.5}$$

where we have labeled $Q^B_{\alpha 0}$ according to the type of transition.

The integrals in Eqs. (4.3) and (4.4) can be evaluated in terms of the modified Bessel functions by making use of the integral

$$\int_0^\infty \frac{\cos(xy)dy}{(y^2 + c^2)^{\nu + 1/2}} = \frac{\pi^{1/2}}{\Gamma(\nu + \frac{1}{2})} \left(\frac{x}{2c}\right)^\nu K_\nu(cx) . \tag{4.6}$$

We obtain from Eq. (4.3)

$$Q^B_{\alpha 0}(b, \sigma \to \sigma) = \frac{ie^2 v_{\rm rel}}{\Delta W} \left(\frac{2^{9+1/2}}{3^5}\right) \zeta^2 \left(K_2(\tau_\sigma) - \frac{2}{\tau_\sigma} K_1(\tau_\sigma)\right) , \tag{4.7}$$

with

$$\tau_\sigma \equiv \zeta (b^2 + a_\sigma^2)^{1/2} . \tag{4.8}$$

Similarly, from Eq. (4.4), we have

$$Q^B_{\alpha 0}(b,\sigma\to\pi)=\pm\frac{ie^2v_{\rm rel}}{\Delta W}\left(\frac{2^8}{3^4}\right)\left(-b\frac{\partial}{\partial\zeta}\int_0^\infty\frac{\cos(\zeta z)\,dz}{(z^2+b^2+a_\pi^2)^{5/2}}\right)=\pm\frac{ie^2v_{\rm rel}}{\Delta W}\left(\frac{2^8}{3^4}\right)\left(-\frac{b}{3(b^2+a_\pi^2)}\frac{\partial}{\partial\zeta}\left[\zeta^2K_2(\zeta(b^2+a_\pi^2)^{1/2})\right]\right). \tag{4.9}$$

The identity

$$\frac{d}{dx}\left[x^2e^{2\pi i}K_2(x)\right]=x^2e^{\pi i}K_1(x) \tag{4.10}$$

reduces Eq. (4.9) to the form

$$Q^B_{\alpha 0}(b,\sigma\to\pi)=\pm\frac{ie^2v_{\rm rel}}{\Delta W}\left(\frac{2^8}{3^5}\right)\frac{b\zeta^3}{\tau_\pi}K_1(\tau_\pi)\,, \tag{4.11}$$

with

$$\tau_\pi\equiv\zeta(b^2+a_\pi^2)^{1/2}\,.$$

The total cross section for the special case of $\delta\Phi_{\alpha 0}=0$ in the eikonal Born approximation can then be obtained from Eq. (2.29). For the $\sigma\to\sigma$ transition, we have

$$\sigma^B_{\alpha 0}(\sigma\to\sigma)=\frac{\pi e^4\zeta^4}{(\Delta W)^2}\left(\frac{2^{20}}{3^{10}}\right)\int_0^\infty b\,db\left(K_2(\tau_\sigma)-\frac{2}{\tau_\sigma}K_1(\tau_\sigma)\right)^2. \tag{4.12}$$

For the $\sigma\to\pi$ transition, we have

$$\sigma^B_{\alpha 0}(\sigma\to\pi)=\frac{\pi e^4\zeta^6}{(\Delta W)^2}\left(\frac{2^{17}}{3^{10}}\right)\int_0^\infty b^3\,db\left(\frac{1}{\tau_\pi}K_1(\tau_\pi)\right)^2. \tag{4.13}$$

In Fig. 3, we have plotted as an example the cross section for the $\sigma-\pi$ transition given by Eq. (4.13) for several values of the constant level spacing ΔW. In this calculation we have taken $a_\pi=1a_0$. It is seen that the cross section drops rapidly with decreasing energy and the over-all magnitude of the cross section decreases with increasing level spacing. This is, of course, expected since the nonadiabatic (or diabatic) effect would increase with a decreased level spacing. For a more relatistic two-state system, the level spacing is generally not constant. We would then expect that the nonadiabatic effect depends on the position and distance of the closest approach of the two adiabatic states.

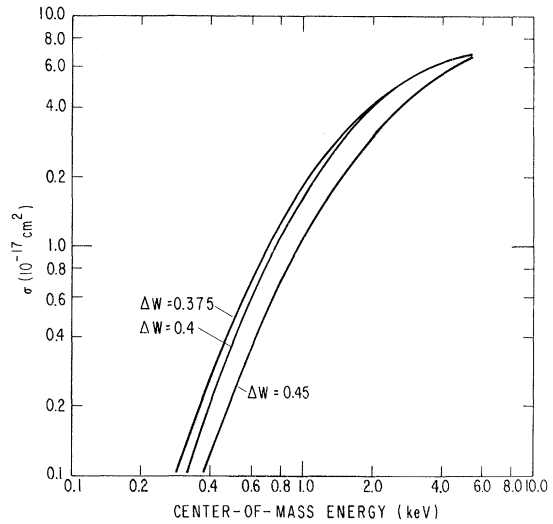

FIG. 3. Variation of cross section with energy for quasiadiabatic transitions between states with constant level spacings as predicted by Eq. (4.13).

B. Two-State Model

Examining Figs. 1 and 2 for the (He^+, H) system, we have found that the level spacings $\Delta w_{\alpha 0}\equiv w_\alpha-w_0$ of these adiabatic electronic states may be reasonably fitted by an analytic function of the type

$$\Delta w_{\alpha 0}(R_1)=\Delta W_{\alpha 0}+\Delta v_{\alpha 0}(R_1)=\Delta W_{\alpha 0}-B_{\alpha 0}/R_1^2+C_{\alpha 0}/R_1^4\,, \tag{4.14}$$

with

$$\Delta W_{\alpha 0}=\lim_{R_1\to\infty}\left[w_\alpha(R_1)-w_0(R_1)\right], \tag{4.15}$$

where $B_{\alpha 0}$ and $C_{\alpha 0}$ are constants. In this subsection, we shall adopt Eq. (4.14) for the level spacings as a model and investigate the qualitative features of the cross section (for quasiadiabatic transitions) as a function of the characteristic parameters of the level spacings. We examine the energy dependence of the cross section on variation in the characteristic parameters, such as the position and distance of closest approach of the levels.

The position and distance of closest approach of the levels for Eq. (4.14) are given, respectively, by

$$R_0=2C_{\alpha 0}/B_{\alpha 0}\,, \tag{4.16}$$

$$(\Delta w_{\alpha 0})_{\rm min}=\Delta W_{\alpha 0}-\tfrac{1}{4}B^2_{\alpha 0}/C_{\alpha 0}\,. \tag{4.17}$$

In Fig. 4, the level spacing $\Delta w_{\alpha 0}(R)$ is displayed for the case where the position of closest approach is taken to be $R_0=5a_0$ and the distance of closest approach is taken to be $\Delta w_{\rm min}=0.1$ a.u.

One of the convenient features of the analytic form of $\Delta w_{\alpha 0}(R)$ given by Eq. (4.14) lies in the fact that the local phase differences $\delta\Phi_{\alpha 0}(\bar{z},b)$ given in Eq. (4.1) can be solved analytically. With the help of the integrals

$$\int_0^x\frac{dy}{y^2+b^2}=\frac{1}{b}\tan^{-1}\left(\frac{x}{b}\right), \tag{4.18}$$

$$\int_0^x\frac{dy}{(y^2+b^2)^2}=\frac{x}{2b^2(x^2+b^2)}+\frac{1}{2b^2}\tan^{-1}\left(\frac{x}{b}\right), \tag{4.19}$$

we obtain for $\delta\Phi_{\alpha 0}(z,b)$

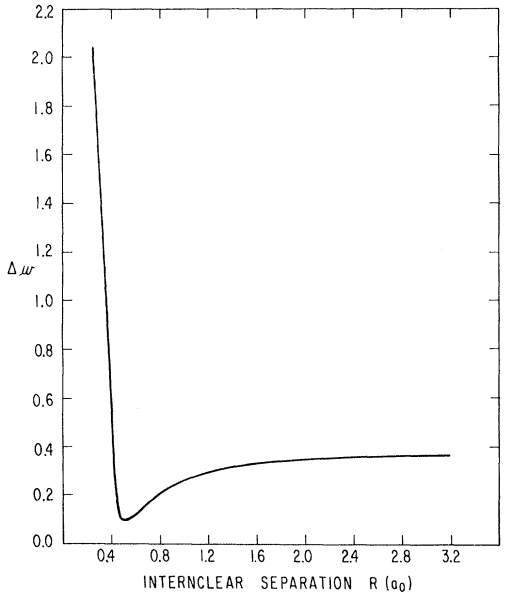

FIG. 4. Example of level spacing vs distance as given by Eq. (4.14) with the position and distance of closest approach of the two states set at $R_0 = 0.5a_0$ and $\Delta w_{\min} = 0.1$ a.u., respectively.

$$\delta\Phi_{\alpha 0}(\bar{z}, b) = \frac{C_{\alpha 0}}{2b^2}\left(\frac{\bar{z}}{\bar{z}^2 + b^2}\right) + \frac{C_{\alpha 0} - b^2 B_{\alpha 0}}{b^3}\tan^{-1}\left(\frac{\bar{z}}{b}\right) . \tag{4.20}$$

Now we are in a position to calculate the quantity $Q^B_{\alpha 0}$ and then the total cross section using Eq. (2.29).

We have carried out a numerical model study of the total cross section for the $\sigma \to \pi$ transition using Eq. (4.20) for the local phase difference and Eq. (3.32) for the nonadiabatic interaction (with $a_\pi = 1a_0$). The results are given in Figs. 5 and 6. In Fig. 5, we have taken the distance of closest approach of the two states to be $\Delta w_{\min} = 0.1$ a.u. and displayed the energy dependence of the cross section for several values of the position of closest approach R_0. It is seen that the cross section is considerably increased at the low-energy side when the position of closest approach is located at a smaller internuclear separation. If we fix the position of closest approach at $R_0 = 1a_0$ and change $\Delta w_{\min}$, we again find that the cross section at the lower-energy side increases when the magnitude of $\Delta w_{\min}$ decreases. This is shown in Fig. 6.

C. Saddle-Point Approximation

The z integral for $Q^B_{\alpha 0}(b)$ given by Eq. (2.25) can also be evaluated using the saddle-point approximation for the two-state model of Sec. IV B. We rewrite Eq. (2.25) as

$$Q^B_{\alpha 0}(b) = \int_{-\infty}^{\infty} dz\, J_{\alpha 0}(z, b)\, e^{i\gamma_{\alpha 0}(z,b)} , \tag{4.21}$$

with

$$\gamma_{\alpha 0}(z, b) = (1/v_{\rm rel}) \int_0^z \Delta w_{\alpha 0}(R)\, dz' , \tag{4.22}$$

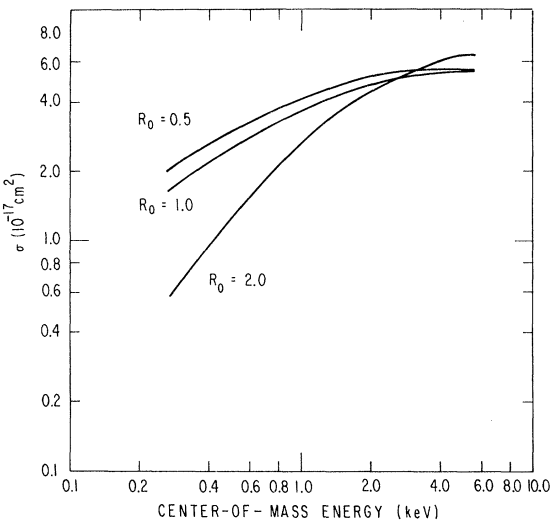

FIG. 5. Effect of varying R_0 (the position of closest approach of the states) on the energy dependence of the cross section for quasiadiabatic transitions between states with a level spacing given by Eq. (4.14). The distance of closest approach of the states was fixed at $\Delta w_{\min} = 0.1$ a.u. The nonadiabatic interaction given by Eq. (3.32) with $a_\pi = 1a_0$ was adopted in the calculation.

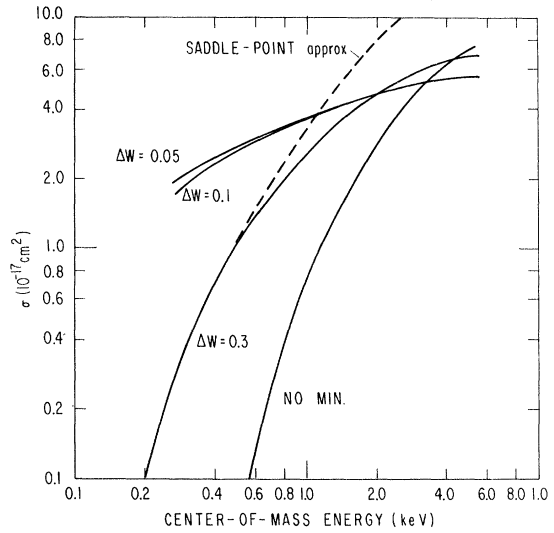

FIG. 6. Effect of varying $\Delta w_{\min}$ (the distance of closest approach of the states) on the energy dependence of the cross section for quasiadiabatic transitions between states with a level spacing given by Eq. (4.14). The position of closest approach of the states was fixed at $R_0 = 1\ a_0$. The nonadiabatic interaction given by Eq. (3.32) with $a_\pi = 1a_0$ was adopted in the calculation.

where we have made use of Eq. (4.5). We assume that the nonadiabatic interaction $J_{\alpha 0}(z, b)$ is a slowly varying function of z so that it can be removed from the integrand in Eq. (4.21):

$$Q^B_{\alpha 0}(b) \cong J_{\alpha 0}(0, b) \int_{-\infty}^{\infty} dz\, e^{i\gamma_{\alpha 0}(z,b)} . \tag{4.23}$$

The integral in Eq. (4.23) can be evaluated by the method of steepest descent.

From Eq. (4.22), we have

$$v_{\rm rel} \frac{d\gamma_{\alpha 0}(z, b)}{dz} = \Delta w_{\alpha 0}(z, b) . \tag{4.24}$$

The saddle point for $\gamma_{\alpha 0}(z, b)$ is therefore the solution of

$$\Delta w_{\alpha 0}(z, b) = 0 . \tag{4.25}$$

To solve Eq. (4.25), we expand $\Delta w_{\alpha 0}$ in a Taylor series around $z = z_0$ ($z_0^2 = R_0^2 - b^2$):

$$\Delta w_{\alpha 0}(z, b) = \Delta w_{\rm min} + \frac{1}{2} \left. \frac{d^2(\Delta w_{\alpha 0})}{dz^2} \right|_{z=z_0} (z - z_0)^2 + \cdots$$

$$\cong [a_1 + a_2(z - z_0)^2]\, v_{\rm rel} , \tag{4.26}$$

with

$$a_1 \equiv \frac{\Delta w_{\rm min}}{v_{\rm rel}} , \quad a_2 \equiv \frac{2B_{\alpha 0}}{v_{\rm rel} R_0^4} \left(1 - \frac{b^2}{R_0^2}\right) . \tag{4.27}$$

When the approximation for $\Delta w_{\alpha 0}$ given by Eq. (4.26) is used, we obtain from Eq. (4.25) the saddle point z_s:

$$z_s = z_0 + (a_1/a_2)^{1/2} e^{i\pi/2} . \tag{4.28}$$

In the neighborhood of the saddle point z_s we have

$$\gamma_{\alpha 0}(z, b) = \gamma_{\alpha 0}(z_s, b) + \frac{1}{2} \left. \frac{d^2\gamma_{\alpha 0}}{dz^2} \right|_{z=z_s} (z - z_s)^2 + \cdots , \tag{4.29}$$

with

$$\gamma_{\alpha 0}(z_s, b) = i\tfrac{2}{3}(a_1^3/a_2)^{1/2} + z_0(a_1 + \tfrac{1}{3}a_2 z_0^2) , \tag{4.30}$$

$$\left. \frac{d^2\gamma_{\alpha 0}}{dz^2} \right|_{z=z_s} = 2(a_1 a_2)^{1/2} e^{i\pi/2} . \tag{4.31}$$

Substitution of $\gamma_{\alpha 0}(z, b)$, which is given by Eq. (4.29), into the integral in Eq. (4.23) yields

$$\int_{-\infty}^{\infty} dz\, e^{i\gamma_{\alpha 0}(z,b)}$$

$$= \frac{4\pi^{1/2}}{(a_1 a_2)^{1/4}} \exp\left[-\frac{2}{3}\left(\frac{a_1^3}{a_2}\right)^{1/2} + iz_0(a_1 + \tfrac{1}{3}a_2 z_0^2)\right] , \tag{4.32}$$

where a factor of 2 was introduced to account for the case where the trajectory passes through the saddle point twice. The condition for validity of the saddle-point integration is that

$$\frac{2}{3}\left(\frac{a_1^3}{a_2}\right)^{1/2} \gg 1 . \tag{4.33}$$

This implies that the transition integral is small. For quasiadiabatic transitions, such integrals are indeed small.

The total cross section given by Eq. (2.29) can now be written in the saddle-point approximation as

$$\sigma_{\alpha 0} \cong \frac{2^5\pi^2}{v_{\rm rel}^2} \int_0^{\infty} b\, db \frac{|J_{\alpha 0}(0, b)|^2}{(a_1 a_2)^{1/2}} \exp\left[-\frac{4}{3}\left(\frac{a_1^3}{a_2}\right)^{1/2}\right] . \tag{4.34}$$

If we further assume that $J_{\alpha 0}$ is also a slowly varying function of b, Eq. (4.34) reduces,[5] after changing the variable to $u^2 = 1 - b^2/R_0^2$, to the approximate form

$$\sigma_{\alpha 0} \approx 3g_0 \left(\frac{4\pi R_0}{a_1 v_{\rm rel}}\right)^2 |J_{\alpha 0}|^2 \int_0^1 \frac{du}{u^2} e^{-2g_0/u} \tag{4.35}$$

$$\approx \frac{16\pi^2 R_0^4}{[2a_1 B_{\alpha 0} v_{\rm rel}^3]^{1/2}} |J_{\alpha 0}|^2 \frac{e^{-2g_0}}{g_0} , \tag{4.36}$$

with

$$g_0 = \frac{R_0^2}{3}\left(\frac{2a_1^3 v_{\rm rel}}{B_{\alpha 0}}\right)^{1/2} = \frac{R_0^2}{3v_{\rm rel}}\left(\frac{2\Delta w_{\rm min}^3}{B_{\alpha 0}}\right)^{1/2} . \tag{4.37}$$

A comparison of the saddle-point approximation with the numerical result is given in Fig. 6 for the case with $\Delta w_{\rm min} = 0.3$ a.u. It is seen that the saddle-point integration of the path integral is reasonably adequate in the regime of quasiadiabatic energies.

D. Comparison of Eikonal Born and Two-State Eikonal Approximations

We now estimate the error introduced by the eikonal Born approximation in a two-state model with the level spacing given by

$$\Delta w_{\alpha 0} = 0.375 - 0.056/(R^2 + 1)^2 \tag{4.38}$$

and the nonadiabatic interaction given by Eq. (3.30). In our estimate of the error, we consider the two-state eikonal approximation [obtained from Eq. (2.62) by taking $N = 2$]

$$\frac{dQ_\alpha}{dz} = \Lambda_{\alpha 0} - i\Lambda_{\alpha 0} Q_0 , \tag{4.39a}$$

$$\frac{dQ_0}{dz} = -i\Lambda_{0\alpha} Q_\alpha \tag{4.39b}$$

to be reasonably accurate. This differs from the eikonal Born approximation in that it allows for the back-and-forth coupling between the two states. If we were to drop the Q_0 term in Eq. (4.39) and solve for Q_α, we would obtain the eikonal Born approximation.

The fractional error in the eikonal Born approximation, $|\sigma - \sigma^B|/\sigma^B$, can now be estimated by solving Eq. (4.39). The result is shown in Fig. 7. It is seen from this figure that the error introduced

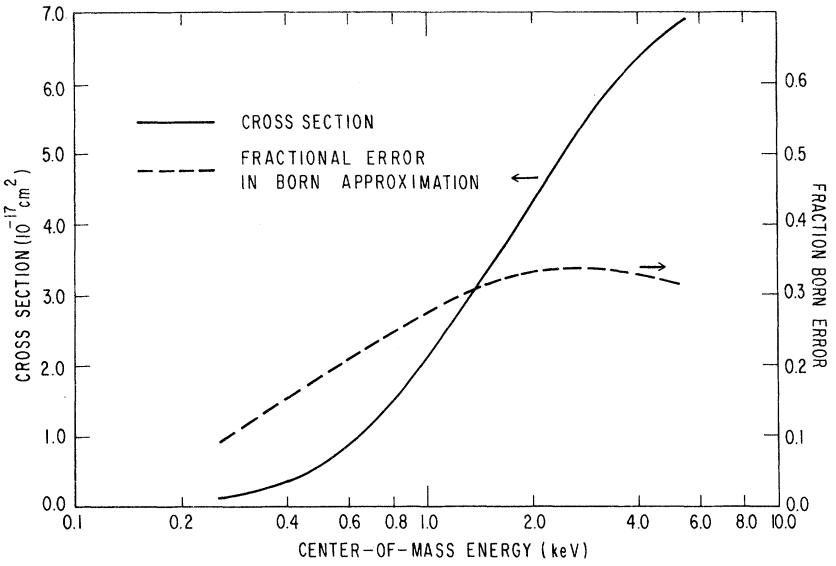

FIG. 7. Estimated errors in the eikonal Born approximation. The solid curve is the cross section obtained in the two state eikonal approximation [Eqs. (4.39)].

by the eikonal Born approximation is reasonably small in the regime of quasiadiabatic energies.

V. MULTISTATE EIKONAL APPROXIMATION FOR $2p$ EXCITATION IN THE (He^+, H) SYSTEM

In this section, we apply the multistate eikonal approximation discussed in Sec. II B to the $2p$ excitation in the (He^+, H) collisions. For the two-electron system, we may treat the singlet and the triplet spin multiplicities separately. For each of the two spin multiplicities, we take into consideration two Σ states and one Π state. The Π state is, of course, doubly degenerate. These states are shown in Figs. 1 and 2. To simplify our notation, we shall label these states in the numerical order 0, 1, 2, and 3, where 0 and 1 denote the initial and final Σ states, respectively, and the degenerate final Π state is denoted as 2 and 3 for $\lambda = +1$ and $\lambda = -1$, respectively.

A. Determination of Excitation Cross Section

In the four-state approximation, we need to solve the following coupled equations [see Eq. (2.62)]:

$$\frac{d}{dz}\begin{pmatrix} Q_0^{(s)} \\ Q_1^{(s)} \\ Q_2^{(s)} \\ Q_3^{(s)} \end{pmatrix} = \begin{pmatrix} 0 \\ \Lambda_{10}^{(s)} \\ \Lambda_{20}^{(s)} \\ \Lambda_{30}^{(s)} \end{pmatrix} - i \begin{pmatrix} 0 & \Lambda_{01}^{(s)} & \Lambda_{02}^{(s)} & \Lambda_{03}^{(s)} \\ \Lambda_{10}^{(s)} & 0 & \Lambda_{12}^{(s)} & \Lambda_{13}^{(s)} \\ \Lambda_{20}^{(s)} & \Lambda_{21}^{(s)} & 0 & \Lambda_{23}^{(s)} \\ \Lambda_{30}^{(s)} & \Lambda_{31}^{(s)} & \Lambda_{32}^{(s)} & 0 \end{pmatrix} \begin{pmatrix} Q_0^{(s)} \\ Q_1^{(s)} \\ Q_2^{(s)} \\ Q_3^{(s)} \end{pmatrix} , \tag{5.1}$$

where the superscript (s) is introduced to denote the spin multiplicity with $s = 1$ for singlet and $s = 3$ for triplet.

Physically it is clear that $Q_0^{(s)}$ accounts for the elastic scattering. The $2p$-excitation amplitude coming from the three final states is given by $Q_1^{(s)}$, $Q_2^{(s)}$, and $Q_3^{(s)}$. Thus, for excitation, we need to solve

$$\begin{aligned} \frac{d}{dz} Q_1^{(s)} &= \Lambda_{10}^{(s)} - i\Lambda_{10}^{(s)} Q_0^{(s)} - i\Lambda_{12}^{(s)} Q_2^{(s)} - i\Lambda_{13}^{(s)} Q_3^{(s)} , \\ \frac{d}{dz} Q_2^{(s)} &= \Lambda_{20}^{(s)} - i\Lambda_{20}^{(s)} Q_0^{(s)} - i\Lambda_{21}^{(s)} Q_1^{(s)} - i\Lambda_{23}^{(s)} Q_3^{(s)} , \\ \frac{d}{dz} Q_3^{(s)} &= \Lambda_{30}^{(s)} - i\Lambda_{30}^{(s)} Q_0^{(s)} - i\Lambda_{31}^{(s)} Q_1^{(s)} - i\Lambda_{32}^{(s)} Q_2^{(s)} . \end{aligned} \tag{5.2}$$

We have observed that the spacings between the initial and any of the three final states are much larger than the spacings among the final states (see Figs. 1 and 2). This suggests that the back coupling of the final states with the initial state should be much smaller than the coupling among the final states. In solving Eqs. (5.2), we shall, therefore, neglect the back coupling with the initial state. Equations (5.2) then reduce to the form

$$\begin{aligned} \frac{d}{dz} Q_1^{(s)} &= \Lambda_{10}^{(s)} - i\Lambda_{12}^{(s)} Q_2^{(s)} - i\Lambda_{13}^{(s)} Q_3^{(s)} , \\ \frac{d}{dz} Q_2^{(s)} &= \Lambda_{20}^{(s)} - i\Lambda_{21}^{(s)} Q_1^{(s)} - i\Lambda_{23}^{(s)} Q_3^{(s)} , \\ \frac{d}{dz} Q_3^{(s)} &= \Lambda_{30}^{(s)} - i\Lambda_{31}^{(s)} Q_1^{(s)} - i\Lambda_{32}^{(s)} Q_2^{(s)} . \end{aligned} \tag{5.3}$$

From the symmetry of the gradient matrix element in the nonadiabatic interaction, and the fact that the final states are close together, we may set

$$\Lambda_{21}^{(s)} \cong -\Lambda_{12}^{(s)} , \quad \Lambda_{31}^{(s)} \cong -\Lambda_{13}^{(s)} . \tag{5.4}$$

For the degenerate Π states 2 and 3, we have

$$\Lambda_{30}^{(s)} = -\Lambda_{20}^{(s)}, \quad \Lambda_{31}^{(s)} = -\Lambda_{21}^{(s)} \tag{5.5}$$

and

$$Q_3^{(s)} = -Q_2^{(s)} , \quad \Lambda_{23}^{(s)} = \Lambda_{32}^{(s)} = 0 . \tag{5.6}$$

When the relations given by Eqs. (5.4)–(5.6) are used, Eq. (5.3) reduces to a pair of coupled equations:

$$\begin{aligned} \frac{d}{dz} Q_1^{(s)} &= \Lambda_{10}^{(s)} - 2\Lambda^{(s)} Q_2^{(s)} , \\ \frac{d}{dz} Q_2^{(s)} &= \Lambda_{20}^{(s)} + \Lambda^{(s)} Q_1^{(s)} , \end{aligned} \tag{5.7}$$

with

$$\Lambda^{(s)} \equiv -i\Lambda_{21}^{(s)} = i\Lambda_{12}^{(s)} = i\Lambda_{31}^{(s)} = -i\Lambda_{13}^{(s)} . \tag{5.8}$$

This pair of coupled equations may be decoupled. We write

$$Q^{(s)} = c_1 Q_1^{(s)} + c_2 Q_2^{(s)} ; \tag{5.9}$$

then from Eq. (5.7)

$$\frac{dQ^{(s)}}{dz} = (c_1\Lambda_{10}^{(s)} + c_2\Lambda_{20}^{(s)}) + \Lambda^{(s)}(c_1 Q_1^{(s)} - 2c_2 Q_2^{(s)}) . \tag{5.10}$$

Now, by requiring

$$c_2 Q_1^{(s)} - 2c_1 Q_2^{(s)} = c_3(c_1 Q_1^{(s)} + c_2 Q_2^{(s)}) \tag{5.11}$$

we obtain

$$c_2 = \pm i\sqrt{2}\, c_1 . \tag{5.12}$$

Upon setting $c_1 = 1$, we obtain

$$Q_\pm^{(s)} = Q_1^{(s)} \pm i\sqrt{2}\, Q_2^{(s)} . \tag{5.13}$$

Equations (5.7) are then decoupled to give

$$\frac{dQ_\pm^{(s)}}{dz} = (\Lambda_{10}^{(s)} \pm i\sqrt{2}\,\Lambda_{20}^{(s)}) \pm i\sqrt{2}\,\Lambda Q_\pm^{(s)} . \tag{5.14}$$

To solve Eqs. (5.14), we let

$$Q_\pm^{(s)} = q_\pm^{(s)} \exp(\pm i\sqrt{2} \int_{-\infty}^{z} \Lambda^{(s)} dz'') . \tag{5.15}$$

Substitution of $Q_\pm^{(s)}$ from Eq. (5.15) into Eq. (5.14) yields

$$\frac{dq_\pm^{(3)}}{dz} = (\Lambda_{10}^{(s)} \pm i\sqrt{2}\,\Lambda_{20}^{(s)}) \exp(\mp i\sqrt{2} \int_{-\infty}^{z} \Lambda^{(s)} dz'') . \tag{5.16}$$

We then obtain for $q_\pm^{(s)}$

$$q_\pm^{(s)} = \int_{-\infty}^{z} dz' [\Lambda_{10}^{(s)}(z', b) \pm i\sqrt{2}\,\Lambda_{20}^{(s)}(z', b)] \times \exp[\pm i\sqrt{2} \int_{-\infty}^{z'} \Lambda^{(s)}(z'', b) dz''] , \tag{5.17}$$

and finally

$$Q_\pm^{(s)} = \int_{-\infty}^{z} dz' [\Lambda_{10}^{(s)}(z', b) \pm i\sqrt{2}\,\Lambda_{20}^{(s)}(z', b)] \times \exp[\mp i\sqrt{2} \int_{z'}^{z} \Lambda^{(s)}(z'', b) dz''] . \tag{5.18}$$

The $2p$-excitation amplitude coming from the final Σ and Π states can now be recovered from $Q_\pm^{(s)}$. We have

$$Q_1^{(s)}(z, b) = \tfrac{1}{2}[Q_+^{(s)}(z, b) + Q_-^{(s)}(z, b)] , \tag{5.19}$$

$$Q_2^{(s)}(z, b) = (i/2\sqrt{2})[Q_-^{(s)}(z, b) - Q_+^{(s)}(z, b)] . \tag{5.20}$$

The partial cross sections for the $1s \to 2p_0$ and $1s \to 2p_{\pm 1}$ excitations of H atom by He^+ ion impact can now be calculated using Eq. (2.63):

$$\sigma_\sigma^{(s)} \equiv \sigma_1^{(s)}(1s \to 2p_0) = 2\pi \int_0^\infty b\, db \left| \lim_{z\to\infty} Q_1^{(s)}(z, b) \right|^2 , \tag{5.21}$$

$$\sigma_\pi^{(s)} \equiv \sigma_2^{(s)}(1s \to 2p_{\pm 1}) = 2\pi \int_0^\infty b\, db \left| \lim_{z\to\infty} Q_2^{(s)}(z, b) \right|^2 . \tag{5.22}$$

The $2p$ excitation is then given by

$$\sigma^{(s)}(1s \to 2p) = \sigma_\sigma^{(s)} + 2\sigma_\pi^{(s)} . \tag{5.23}$$

We then obtain for the total cross section

$$\sigma(1s - 2p) = \tfrac{1}{4}\sigma^{(1)} + \tfrac{3}{4}\sigma^{(3)} . \tag{5.24}$$

B. Numerical Results

For the evaluation of the amplitude $Q_1^{(s)}(b)$ and $Q_2^{(s)}$, we need the energy differences between every two states. From our model (He^+, H) potentials given in Figs. 1 and 2, it is seen that the potential difference between the $A\,^1\Sigma$ and $E\,^1\Sigma$ HeH^+ states is not appreciably different from that between the $A\,^1\Sigma$ and $C\,^1\Pi$ states. This is also the case for the $(a\,^2\Sigma, f\,^3\Sigma)$ and $(a\,^3\Sigma, e\,^3\Pi)$ pairs. In view of the uncertainties in these model potentials, we shall assume them to be equal:

$$\Delta\mathcal{U}_{10}^{(1)} = \Delta\mathcal{U}_{20}^{(1)} , \quad \Delta\mathcal{U}_{10}^{(3)} = \Delta\mathcal{U}_{20}^{(3)} . \tag{5.25}$$

These potential differences, which are shown in Fig. 8, can be fitted analytically by the forms

$$\Delta\mathcal{U}_{10}^{(1)} = \frac{2.16}{(R^2+1.99)} - \frac{10.94}{(R^2+1.99)^2} + \frac{2.21}{(R^2+1.06)^3} , \tag{5.26}$$

$$\Delta\mathcal{U}_{10}^{(3)} = \frac{2.26}{(R^2+0.83)} - \frac{8.0}{(R^2+0.83)^2} + \frac{7.35}{(R^2+0.94)^3} . \tag{5.27}$$

This then permits the phases $\phi_{\beta 0}^{(s)}$ in $\Lambda_{\alpha 0}^{(s)}$ [see Eq. (2.53)] to be evaluated analytically as shown in Sec. IV B.

The equality assumed in Eq. (5.25) implies that

$$\phi_{10}^{(s)} = \phi_{20}^{(s)} . \tag{5.28}$$

Consequently, we have from Eqs. (5.18)–(5.20)

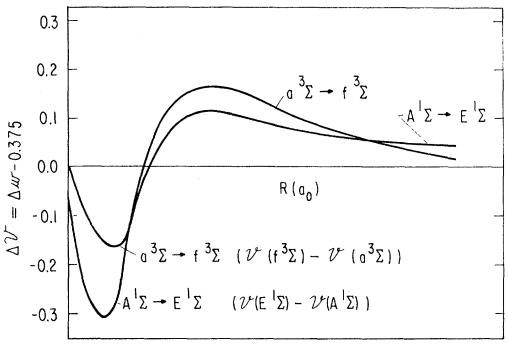

FIG. 8. Energy-level difference assumed between the $A\,^1\Sigma$ and $E\,^1\Sigma$ singlet adiabatic HeH^+ states between the $a\,^3\Sigma$ and $f\,^3\Sigma$ triplet adiabatic HeH^+ states. These energy-level differences are adopted for the calculation reported in subsequent figures (Figs. 9–12).

$$Q_1^{(s)}(z, b) = \frac{1}{v_{\rm rel}} \int_{-\infty}^{z} dz' \,[J_{10}\cos(\delta q_{12}^{(s)}) - \sqrt{2}\, J_{20}\sin(\delta q_{12}^{(s)})]\, e^{i\phi_{10}^{(s)}}, \quad (5.29)$$

$$Q_2^{(s)}(z, b) = \frac{1}{v_{\rm rel}} \int_{-\infty}^{z} dz' \,[2^{-1/2} J_{10}\sin(\delta q_{12}^{(s)}) + J_{20}\cos(\delta q_{12}^{(s)})]\, e^{i\phi_{10}^{(s)}}, \quad (5.30)$$

with

$$\delta q_{12}^{(s)}(z, z') \equiv \sqrt{2} \int_{z'}^{z} \Lambda^{(s)}(z'', b)\, dz'', \quad (5.31)$$

where $\delta q_{12}^{(s)}$ is the local final-state coupling amplitude.

In view of the assumed equality given by Eq. (5.25), the potential difference between final states may be taken to be zero. This, together with the fact that these final states are asymptotically degenerate, allows $\delta q_{12}^{(s)}$ to take the approximate form [see Eqs. (2.50), (2.53), and (5.8)]

$$\delta q_{12}^{(s)}(z, z') \cong \sqrt{2}/v_{\rm rel} \int_{z'}^{z} J_{12}(2p_0 \rightarrow 2p_{\pm 1})\, dz'' . \quad (5.32)$$

When Eq. (3.33) for the nonadiabatic interaction is adopted in Eq. (5.32), we obtain, in the $z \rightarrow \infty$ limit, the simple results

$$\delta q_{12}^{(1)}(\infty, z') \cong \frac{180}{(b^2 + a_{\pi 1}^2)^{1/2}} \frac{bz'}{(z'^2 + b^2 + a_{\pi 1}^2)^{5/2}}, \quad (5.33)$$

$$\delta q_{12}^{(3)}(\infty, z') \cong \frac{360}{(b^2 + a_{\pi 1}^2)^{1/2}} \frac{bz'}{(z'^2 + b^2 + a_{\pi 1}^2)^{5/2}}, \quad (5.34)$$

where we have taken $\Delta w_{12}^{(1)} = 0.1$ and $\Delta w_{12}^{(3)} = 0.05$. We note that these are not the asymptotic values but are reasonable approximations in the required R range (see Figs. 1 and 2).

Calculations were carried out using Eqs. (5.29), (5.30), (5.33), and (5.34) with the nonadiabatic interactions J_{10} and J_{20} approximated by Eqs. (3.31) and (3.32), respectively. In this calculation, we have taken $a_\sigma = a_\pi = a_{\pi 1} = 1.2a_0$ for the nonadiabatic interactions. The calculated cross sections are not sensitive to variation within 20% of the a's. The result for the total $2p$-excitation cross section [see Eq. (5.24)] is compared with experimental measurements[6] in Fig. 9. It is seen that the agreement is remarkable in view of the approximations that we have adopted in the calculation. For comparison, we have also included in Fig. 9 the result obtained in the eikonal Born approximation without final-state interactions. It is seen that the coupling

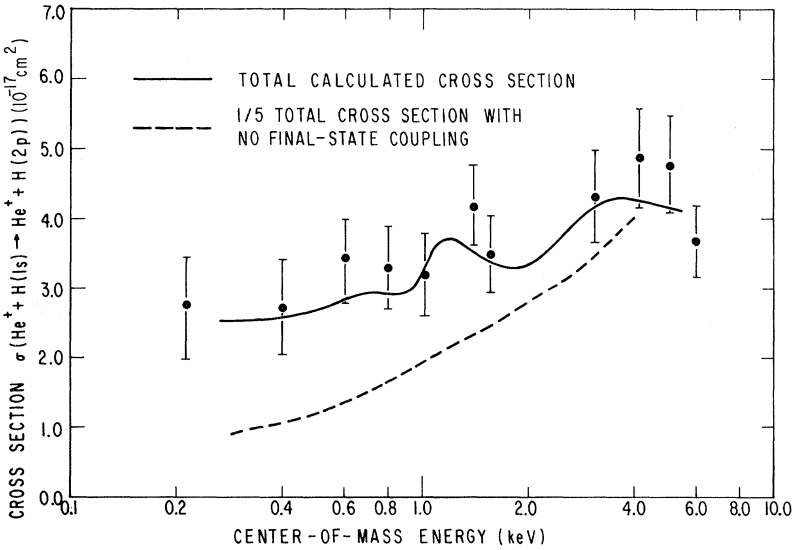

FIG. 9. Comparison of the energy dependence of the $2p$-excitation cross section in the eikonal Born and multistate eikonal approximation with experimental measurements (Ref. 6). The dashed curve is obtained in the eikonal Born approximation in which the coupling of final states is not considered.

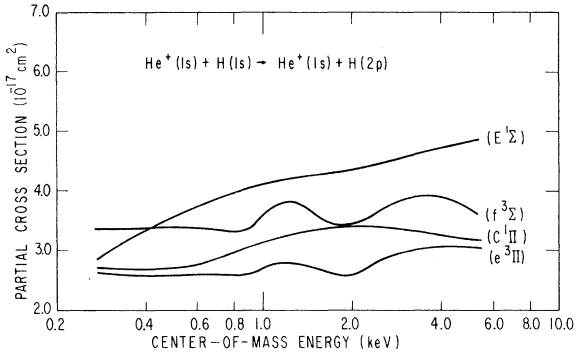

FIG. 10. Energy dependence of the partial $2p$-excitation cross sections coming from each of the four final states considered in the calculation.

of the final states is extremely important.

The contributions to the $2p$-excitation cross section coming from each of the four final states are shown in Fig. 10. In general the $\sigma \to \sigma$ transitions have a larger magnitude than the $\sigma \to \pi$ transitions. To test the sensitivity of our results on the approximation adopted for the local final-state coupling amplitude $\delta q_{12}^{(s)}$, we have repeated our calculation for different values of $\delta q_{12}^{(s)}$ as shown in Fig. 11.

C. Polarization of Emitted Radiation

The probability of an atom undergoing a transition from state a to b and emitting light into a solid angle $d\Omega$ per unit time is

$$W_{ba}(\Omega)d\Omega = \frac{e^2\omega_{ba}}{2\pi\hbar m^2 c^3}\sum_j |\langle b|\vec{p}\cdot\hat{e}_j|a\rangle|^2 d\Omega = \frac{e^2\omega_{ba}^3}{2\pi\hbar c^3}\sum_j |\langle b|\vec{d}\cdot\hat{e}_j|a\rangle|^2 d\Omega , \quad (5.35)$$

with

$$\omega_{ba} \equiv ck = (W_b - W_a)/\hbar , \quad (5.36)$$

where c is the velocity of light and $\vec{d}$ is the dipole vector. The intensity of the light so emitted is given by

$$I_{ba}(\theta) = \frac{e^2\omega_{ba}^4}{2\pi c^3}\sum_j |\langle b|\vec{d}\cdot\hat{e}_j|a\rangle|^2 . \quad (5.37)$$

The sum in Eqs. (5.35) and (5.37) sums over the polarization direction $\hat{e}_j$.

For a $2p \to 1s$ transition, the intensity is given by a sum of contributions coming from the $2p_0 \to 1s$ and $2p_{\pm 1} \to 1s$ transitions:

$$I(\theta) = I(\theta, 2p_0 \to 1s) + 2I(\theta, 2p_\pm \to 1s) . \quad (5.38)$$

The intensity of light emitted for a $2p_0 \to 1s$ transition is

$$I(\theta, 2p_0 \to 1s) = \frac{e^2\omega_{21}^4}{2\pi c^3}\mathcal{P}_0\left(|\langle 2p_0|\vec{d}|1s\rangle|^2 - k^{-2}|\langle 2p_0|\vec{d}\cdot\vec{k}|1s\rangle|^2\right) = \frac{e^2\omega_{21}^4 d_0^2}{2\pi c^3}\mathcal{P}_0(1-\cos^2\theta) , \quad (5.39)$$

where $\mathcal{P}_0$ is the probability of the atom being in the $2p_0$ state. Similarly, the intensity of the light emitted for the $2p_{\pm 1} \to 1s$ transition is

$$I(\theta, 2p_{\pm 1} \to 1s) = \frac{e^2\omega_{21}^4}{2\pi c^3}\mathcal{P}_\pm\left(|\langle 2p_{\pm 1}|\vec{d}|1s\rangle|^2 - k^{-2}|\langle 2p_{\pm 1}|\vec{d}\cdot\vec{k}|1s\rangle|^2\right) = \frac{e^2\omega_{21}^4 d_0^2}{2\pi c^3}\mathcal{P}_{\pm\frac{1}{2}}(1+\cos^2\theta) , \quad (5.40)$$

where $\mathcal{P}_\pm$ is the probability of the atom being in the $2p_{\pm 1}$ state.

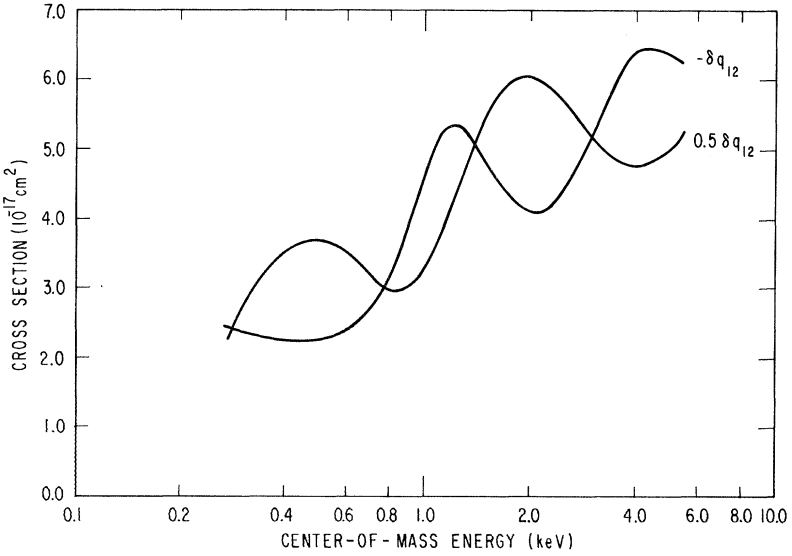

FIG. 11. Effect of varying the local final-state coupling amplitude $\delta q_{21}^{(3)}$ on the energy dependence of $2p$-excitation cross section.

Substitution of Eqs. (5.39) and (5.40) into Eq. (5.38) yields for the intensity

$$I(\theta)=\frac{e^2\omega_{21}^4}{2\pi c^3}\, d_0^2(\mathcal{P}_0+\mathcal{P}_\pm)\,(1-P\cos^2\theta)\,, \qquad (5.41)$$

with

$$P=\frac{\mathcal{P}_0-\mathcal{P}_\pm}{\mathcal{P}_0+\mathcal{P}_\pm}\,, \qquad (5.42)$$

where P is the polarization which can be experimentally measured.

The polarization of the light emitted from the $2p$ state of an H atom excited by He^+ impact can be calculated from the partial cross sections $\sigma_1^{(s)}$ and $\sigma_2^{(s)}$ for the $2p_0$ and $2p_\pm$ states, respectively. We have for the probabilities

$$\mathcal{P}_0=\frac{\frac{1}{4}\sigma_1^{(1)}+\frac{3}{4}\sigma_1^{(3)}}{\sigma}\,, \quad \mathcal{P}_\pm=\frac{\frac{1}{4}\sigma_2^{(1)}+\frac{3}{4}\sigma_2^{(3)}}{\sigma}\,, \qquad (5.43)$$

where σ is the total cross section given by Eq. (5.24). This then yields for the polarization

$$P=\frac{(\sigma_1^{(1)}-\sigma_2^{(1)})-3(\sigma_1^{(3)}-\sigma_2^{(3)})}{(\sigma_1^{(1)}+\sigma_2^{(1)})+3(\sigma_1^{(3)}+\sigma_2^{(3)})}\,. \qquad (5.44)$$

We have plotted in Fig. 12 the calculated polarization of Eq. (5.44) using the partial cross sections given in Fig. 10. For comparison we have also included in Fig. 12, the polarization based on the partial cross sections which are calculated without allowing for the final-state coupling. The theoretical results (including final-state coupling) are larger than the experimentally estimated magnitude[6] by approximately a factor of 2.

APPENDIX A: CLASSICAL LIMIT OF MULTISTATE EIKONAL APPROXIMATION

The inelastic transition amplitude in the multistate eikonal approximation given by Eqs. (2.56) and (2.57) can be rewritten as

$$T_{\alpha 0}^{(N)}=(2\pi)^{-2}\sum_{\beta\neq\alpha}^{N}\int_0^\infty b\,db\,J_0(kb\sin\theta)\,Q_{\alpha\beta}^{(2)}(b)\,e^{(i/2)\Phi_{\alpha\beta}(b)}\,, \qquad (A1)$$

with

$$Q_{\alpha\beta}^{(2)}(b)=\int_{-\infty}^{\infty}dz'\,J_{\alpha\beta}(z',b)\,e^{i\tilde{\phi}_{\alpha\beta}(z',b)}\,\gamma_\beta(z',b)\,, \qquad (A2)$$

$$\tilde{\phi}_{\alpha\beta}(z',b)=\tfrac{1}{2}[\Phi_\alpha(b)-\Phi_\beta(b)]-\phi_{\alpha\beta}(z',b)\,, \qquad (A3)$$

where Eq. (A2) reduces to Eq. (2.25) for $\beta=0$ if γ_0 is set equal to unity. Equation (A1) resembles the familiar eikonal approximation of Molière for potential scattering [see Eq. (II5.11)]. The generalization of the eikonal approximation to multichannel scattering give rise to the factors $Q_{\alpha\beta}^{(2)}$ to account for transitions between states. A classical limit of Eq. (A1) may be obtained in a manner similar to that for Molière's expression.

The error resulting from the classical description of the collisions is of order [Eqs. (II5.19) and (II1.25)]

$$\eta_{(\mathrm{class})}=\frac{d^2\Theta_c}{db^2}\left(k^{1/2}\left|\frac{d\Theta_c}{db}\right|^{3/2}\right)^{-1}\sim\left(\frac{E}{920A_{\mathrm{eff}}}\right)^{1/2}\,, \qquad (A4)$$

where Θ_c is the classical scattering angle defined in terms of the appropriate phase. For the present problem, the classical scattering angle is defined in terms of $\frac{1}{2}\Phi_{\alpha\beta}$ [see Eq. (2.22)]:

$$M_r\,v_\beta\Theta_{c\beta}(b)=\frac{1}{2}\frac{\partial}{\partial b}\Phi_{\alpha\beta}(b)=\frac{1}{2}\left(\frac{\partial}{\partial b}\Phi_\alpha(b)+\frac{\partial}{\partial b}\Phi_\beta(b)\right) \qquad (A5)$$

On using the asymptotic form for the Bessel function

$$J_0(kb\sin\theta)\cong\left(\frac{2}{\pi kb\sin\theta}\right)^{1/2}\cos(kb\theta-\tfrac{1}{4}\pi)\,, \qquad (A6)$$

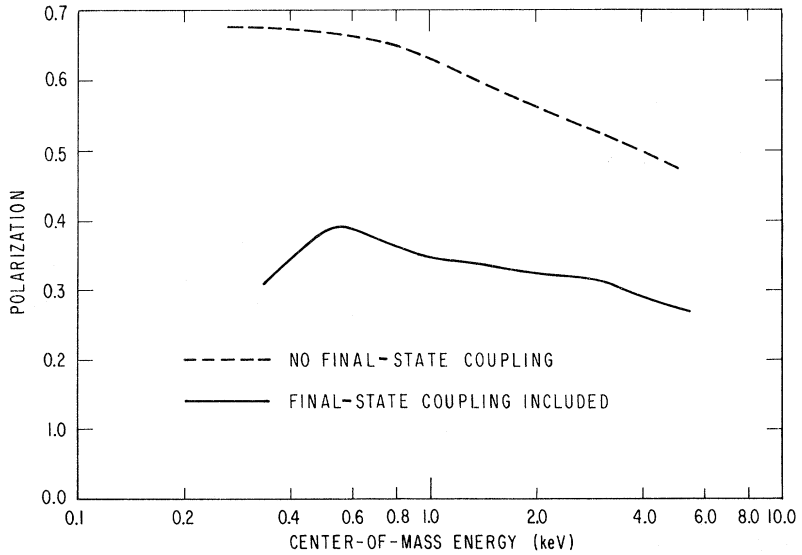

FIG. 12. Comparison of the energy dependence of the calculated polarization of emitted radiation in the eikonal Born and multistate eikonal approximations. The dashed curve is obtained in the eikonal Born approximation in which the coupling of final states is not considered.

we may rewrite Eq. (A1) as

$$T_{\alpha 0}^{(N)} \cong \frac{1}{8\pi^2}\left(\frac{2}{\pi k b \sin\theta}\right)^{1/2} \sum_{\beta\neq\alpha}^{N} \int_0^\infty db\, b^{1/2} Q_{\alpha\beta}^{(2)}(b) \times e^{i\gamma_{\alpha\beta}(b)+ie_\beta\pi/4}, \quad \text{(A7)}$$

with

$$e_\beta(b) \equiv \Theta_{c\beta}(b)/|\Theta_{c\beta}(b)|, \quad \text{(A8)}$$

$$\gamma_{\alpha\beta}(b) \equiv \tfrac{1}{2}\Phi_{\alpha\beta}(b) - e_\beta(kb\theta). \quad \text{(A9)}$$

The integral of Eq. (A7) can be evaluated in the stationary-phase approximation.

The stationary-phase point at $b = b_{c\beta}$ is obtained from

$$\frac{d\gamma_{\alpha\beta}(b_{c\beta})}{db} = M_r v_\beta(\Theta_{c\beta}(b_{c\beta}) - e_1\theta) = 0. \quad \text{(A10)}$$

This then defines $b_{c\beta}$ as

$$\theta = |\Theta_{c\beta}(b_{c\beta})|. \quad \text{(A11)}$$

In the neighborhood of $b_{c\beta}$

$$\gamma_{\alpha\beta}(b) = \gamma_{\alpha\beta}(b_{c\beta}) + \frac{M_r v_\beta}{2}\frac{d\Theta_{c\beta}(b_{c\beta})}{db}(b - b_{c\beta})^2 + O[\eta(\text{class})]. \quad \text{(A12)}$$

A stationary-phase evaluation of Eq. (A7) leads to the classical limit of $T_{\alpha 0}^{(N)}$

$$T_{\alpha 0}^{(N)} \cong \frac{i}{(2\pi)^2 M_r}\sum_{\beta\neq\alpha}^{N}\frac{1}{v_\beta}\left(\frac{b_{c\beta}}{\sin\theta}\left|\frac{db_{c\beta}}{d\Theta_{c\beta}}\right|\right)^{1/2} \times Q_{\alpha\beta}^{(2)}(b_{c\beta})\, e^{i\gamma_{\alpha\beta}(b_{c\beta})+ie'_\beta/4}, \quad \text{(A13)}$$

with

$$e'_\beta = e_\beta(b_{c\beta}) - 2 + \frac{d\Theta_{c\beta}/db_{c\beta}}{|d\Theta_{c\beta}/db_{c\beta}|}. \quad \text{(A14)}$$

This then leads to the multistate classical approximation for the cross section

$$\frac{d\sigma}{d\Omega} \cong \frac{v_k}{v_p}\left|\sum_{\beta\neq\alpha}^{N}\frac{1}{v_\beta}\left(\frac{b_{c\beta}}{\sin\theta}\left|\frac{db_{c\beta}}{d\Theta_{c\beta}}\right|\right)^{1/2} \times Q_{\alpha\beta}^{(2)}(b_{c\beta})e^{i\gamma_{\alpha\beta}(b_{c\beta})+i\pi e'_\beta/4}\right|^2. \quad \text{(A15)}$$

For the case with $N=2$, Eq. (A15) reduces to

$$\frac{d\sigma}{d\Omega} \cong \frac{v_k}{v_p^2}\left\{\frac{b_{c0}}{\sin\theta}\left|\frac{db_{c0}}{d\Theta_{c0}}\right|\right\}|Q_{\alpha 0}^{(2)}(b_{c0})|^2. \quad \text{(A16)}$$

The classical limit of the eikonal Born approximation is given by Eq. (A16) with $Q_{\alpha 0}^{(2)}(b_{c0})$ replaced by $Q_{\alpha 0}^{B}(b_{c0})$ [see Eq. (2.25)].

APPENDIX B: ANALYTIC MODEL HeH^+ ADIABATIC POTENTIALS

The set of model He H^+ adiabatic potentials shown in Fig. 1 can be represented by the following analytic forms (in hartree units):

$$(A\,^1\Sigma)\quad V(R) = -2.5 + (2/R)e^{-1.2736R} + 6.987R^2 e^{-2.3444R} - 8.9285\times10^{-3}R\,e^{-0.62023R},$$

$$(C\,^1\Pi)\quad V(R) = -2.125 + (2/R)\,e^{-1.2977R} + 0.3R^2 e^{-1.2R} - 5.999\times10^{-3}R\,e^{-0.22116R},$$

$$(E\,^1\Sigma)\quad V(R) = -2.125 + (2/R)\,e^{-1.2986R} + 2.5R^2 e^{-1.85R} + 0.06407R\,e^{-0.3041R},$$

$$(a\,^3\Sigma)\quad V(R) = -2.5 + (2/R)\,e^{-1.3055R} + 9.3077R^2 e^{-2.8549R} - 1.6254\times10^{-2}R\,e^{-0.68464R},$$

$$(e\,^3\Pi)\quad V(R) = -2.125 + (2/R)\,e^{-1.3028R} + 0.625\,e^{-0.40236R},$$

$$(f\,^3\Sigma)\quad V(R) = -2.125 + (2/R)\,e^{-1.3028R} + 0.42875\,e^{-0.31319R}.$$

These potentials $[V(R) \equiv w(R) = W + \mathcal{U}(R)]$ reproduce reasonably well the calculated values of Michels[4] at intermediate internuclear separations and go over to the exact united and separated atom limits indicated in Table I.

APPENDIX C: NONADIABATIC INTERACTION BETWEEN FINAL STATES

The nonadiabatic interaction between the final Σ and Π states in the asymptotic region vanishes to order R^{-3}. We must therefore consider the higher-order terms in Eq. (3.19). By utilizing the expansion

$$|\vec{R}_1 + \vec{q}|^{-3} = R_1^{-3}\left[1 - \left(3\frac{\hat{R}_1\cdot\vec{q}}{R_1} - \frac{3}{2}\left(\frac{q}{R_1}\right)^2 + \frac{15}{2}\frac{(\hat{R}_1\cdot\vec{q})^2}{R_1^2} + \cdots\right)\right], \quad \text{(C1)}$$

we obtain from Eqs. (3.11)–(3.14)

$$(\nabla_{R_1} h_a) = \frac{2e^2\hat{R}_1}{R_1^2} + \frac{e^2}{R_1^3}[\vec{r}_1 - 3\hat{R}_1(\hat{R}\cdot\vec{r}_1)] + \frac{3e^2}{R_1^4}\left[\tfrac{5}{2}\hat{R}_1(\hat{R}_1\cdot\vec{r}_1)^2 - \tfrac{1}{2}\hat{R}r_1^2 - \vec{r}_1(\hat{R}\cdot\vec{r}_1) + 5(\hat{R}_1\cdot\vec{r}_1)(\hat{R}_1\cdot\vec{r}_2) - \vec{r}_1(\hat{R}_1\cdot\vec{r}_2) - \vec{r}_2(\hat{R}_1\cdot\vec{r}_1) - \tfrac{1}{2}\hat{R}_1(\vec{r}_1\cdot\vec{r}_2)\right] + O(R^{-5}). \quad \text{(C2)}$$

Because the helium-ion electron 2 is tightly bound to He^{++}, we may neglect the contributions coming

from electron 2. The matrix element in Eq. (3.29) then takes the form

$$g(2p_0 \rightarrow 2p_{\pm 1}) = (R^{H}_{2p}(r_1) Y_1^{\pm 1}(\hat{r}_1),\ \hat{k}\cdot[\tfrac{15}{2}\hat{R}_1(\hat{R}_1\cdot\vec{r}_1)^2 - \tfrac{3}{2}\hat{R}r_1^2 - 3\vec{r}_1(\hat{R}\cdot\vec{r}_1)]\, R^{H}_{2p}(r_2) Y_1^0(\hat{r}_1))\ . \tag{C3}$$

We have

$$(Y_1^{-1}(\hat{r}_1),\ (\hat{R}_1\cdot\vec{r}_1)^2\, Y_1^0(\hat{r}_1)) = r_1^2 \int Y_1^{-1}(\hat{r}_1)^*\,[\cos\gamma\cos\theta_1 + \sin\gamma\cos\theta_1\cos\varphi_1]^2\, Y_1^0(\hat{r}_1)\, d\hat{r}_1 = (\sqrt{2}/5)\, r^2\cos\gamma\sin\gamma\ , \tag{C4}$$

$$(Y_1^{-1}(\hat{r}_1),\ (\hat{k}\cdot\vec{r}_1)(\hat{R}_1\cdot\vec{r}_1) Y_1^0(\hat{r}_1)) = r_1^2 \int Y_1^{-1}(\hat{r}_1)^*\cos\theta_1[\cos\gamma\cos\theta_1 + \sin\gamma\sin\theta_1\cos\varphi_1]\, Y_1^0(\hat{r}_1)\, d\hat{r}_1 = r^2\sin\gamma/5\sqrt{2}\ . \tag{C5}$$

This then leads to

$$g(2p_0 \rightarrow 2p_{\pm 1}) = (3/\sqrt{2})\sin\gamma\,[\cos^2\gamma - \tfrac{1}{5}] \times (R^{H}_{2p}(r_1),\ r_1^2 R^{H}_{2p}(r_1))\ , \tag{C6}$$

which is equivalent to Eq. (3.30).

*Research supported in part by the National Science Foundation Grant No. GP-20459, by the Atomic Energy Commission Contract No. AT(04-3)-34, PA196, and by the U. S. Air Force Office of Scientific Research Grant No. F44620-C-70-0028.

†Present address: Physique Théorique et Mathématique, Faculté des Sciences, Université Libre de Bruxelles, Brussels, Belgium.

[1]J. C. Y. Chen and K. M. Watson, Phys. Rev. 174, 152 (1968). Equations from Paper I will be referred to as, e.g., Eq. (I1.1), etc.

[2]J. C. Y. Chen and K. M. Watson, Phys. Rev. 188, 236 (1969). Equations from Paper II will be referred to as, e.g., Eq. (II1.1), etc.

[3]J. C. Y. Chen, C.-S. Wang, and K. M. Watson, Phys. Rev. A 1, 1150 (1970).

[4]H. H. Michels, J. Chem. Phys. 44, 3834 (1966).

[5]K. M. Watson, in *Properties of Matter Under Unusual Conditions*, edited by H. Mark and S. Fernbach (Wiley, New York, 1969), p. 327.

[6]R. A. Young, R. F. Stebbings, and J. W. McGowan, Phys. Rev. 171, 85 (1968).

[7]K. M. Watson, Phys. Rev. 88, 1163 (1952).

[8]K. M. Watson and J. C. Y. Chen, in *Proceedings of the Seventh International Conference on the Physics of Electronic and Atomic Collisions* (North-Holland, Amsterdam, 1971), p. 448.

[9]This approximation may be easily relaxed.

[10]H. Tai, R. H. Bassel, E. Gerjuoy, and V. Franco, Phys. Rev. A 1, 1819 (1970).

[11]J. C. Y. Chen, C. J. Joachain, and K. M. Watson, Phys. Rev. A (to be published).

PHYSICAL REVIEW A VOLUME 5, NUMBER 3 MARCH 1972

Deduction of Heavy-Ion X-Ray Production Cross Sections from Thick-Target Yields

Knud Taulbjerg
Institute of Physics, University of Aarhus, 8000 Aarhus, Denmark

and

Peter Sigmund
Physical Laboratory II, H. C. Ørsted Institute, DK-2100, Copenhagen, Denmark

(Received 26 October 1971)

The conventional formula determining x-ray production cross sections from thick-target yields has to be corrected for the effects of energy-loss straggling, x rays from recoil atoms, and nonstraight ion trajectories when heavy (keV and low MeV) ions are used as projectiles. The first two corrections are evaluated in this paper for the case where the last is small (negligible absorption). Carbon K x-ray cross sections are deduced from published yield data. Large corrections, up to one order of magnitude, are found.

I. INTRODUCTION

When heavy ions slow down in gaseous or solid targets inner-shell excitations are created in violent collisions even at velocities $v < e^2/\hbar$.[1] Characteristic x-ray production cross sections σ_x of the order of up to almost 10^5 b have been reported.[2,3] As a function of ion energy E, the reported cross sections rise steeply from a rather well-defined threshold energy[2,4] U. At higher energies, σ_x increases more slowly with energy. Eventually, a dropoff of σ_x at still higher energies must be expected, similar to the case of light ions at velocities[5] $v \gg e^2/\hbar$.

Experimentally, cross sections were determined either directly, in gas targets under single-collision